[redacted] UNCLASSIFIED

THIS DOCUMENT HAS BEEN DOWNGRADED
TO UNCLASSIFIED MAR 23 1993
Per Director, ARPA, S+IO/TIO

~~Classified by DD 254, 10-1-78, Contract F19628-78-C-0001 and 4140 Security Guide dated April 1976.~~
~~Exempt from general declassification schedule of Executive Order 11652.~~
~~Exemption category 3.~~
Declassify on *Dec. 31, 1991*

The Enigma of the AN/FPS–95 OTH Radar (U)

E. N. Fowle, E. L. Key, R. I. Millar, and R. H. Sear

The MITRE Corporation, Bedford, Mass.

(Received May 22, 1979)

(U) ~~(S)~~ Cobra Mist, the AN/FPS–95 over-the-horizon (OTH) radar built on the English North Sea Coast in the late 1960's to overlook air and missile activity in Eastern Europe and the western areas of the USSR, was the most powerful and sophisticated radar of its kind up to that time. The design, which emulated Naval Research Laboratory's Madre over-the-horizon radar, incorporated rather coarse spatial resolution and relied upon ultralinear, wide dynamic range components and complex signal processing in attempting to achieve the extreme subclutter visibility (SCV) of 80 to 90 dB needed to separate target returns from the strong ground clutter—a goal well beyond the 60-odd decibel subclutter visibility previously achieved. The detection performance of the radar was spoiled, however, because the actual subclutter visibility achieved was only 60 to 70 dB, the limitation being due to a noise with approximately flat amplitude-versus-Doppler frequency, which appeared in all range bins containing ground clutter and aircraft returns. Experiments performed at the site failed to uncover the source of the noise, either in the equipment or in the propagation medium. Other experimental results imply that the noise was associated with returns from land areas and not from sea surfaces; the possibility of electronic countermeasures was not ruled out. Because the source of the noise was not located and corrected, the radar program was terminated in June 1973 and the equipment removed from the site. The cause of the noise is unknown to this day.

INTRODUCTION

This is as strange a maze as e'er men trod;
And there is in this business more than nature
Was ever conduct of: some oracle
Must rectify our knowledge.

Shakespeare (The Tempest)

(U) ~~(S)~~ This paper recounts the story of Cobra Mist, the AN/FPS–95 over-the-horizon radar built in England on the North Sea Coast in the late 1960's and operated there until mid-1973, when the program was discontinued.

(U) ~~(S)~~ As many will remember, the AN/FPS–95 was the largest, most powerful, and most sophisticated OTH (over-the-horizon) radar of its time; and the OTH community as a whole had high hopes that in performance and capability Cobra Mist would set new standards for the OTH radar art. Quite the opposite happened, however. The radar was plagued from the beginning by difficulties, and although the problems within the equipment itself—which were never very serious—were tracked down and corrected, a residual problem, apparently in the external environment, seriously impaired the detection performance of the radar and led ultimately to the discontinuance of the program. The source of the difficulty that caused Cobra Mist's demise was never found. At the conclusion of the program a rather extensive set of reports on the program([1]) were prepared for the U.S. Air Force, but these were not widely distributed. Consequently, the community did not benefit fully from the AN/FPS–95 experience.

(U) ~~(S)~~ The authors of this paper were all in some way intimately associated with the AN/FPS–95, both in its initial operational phases and in the final phase when an all-out, though time-limited, attempt was made to locate and correct the critical difficulty. The point of this paper is to give an account of the final phase: to list the

*(U) ~~The markings NOFORN and NF used in this paper have been derived from the source material.~~

possible causes of the radar's poor performance and to describe the evidence for and against those causes as gathered through measurements and tests conducted at the site.

(U) {(S)} The paper begins with a brief history of the AN/FPS-95 program, its origins, the design basis, factors that led to the choice of a site in England, and the essential features of the difficulties that led to program termination. Following that is a careful description of the radar system itself, equipment components and all. Next is a discussion of the radar's capabilities and limitations, both those that were expected and those that were actually observed; the nature of the principal difficulty, the so-called "clutter-related noise," is then described. The last three sections treat, in turn, some possible causes for the noise: in the radar equipment itself, in the external environment in general, and in postulated countermeasure activities. The evidence is reviewed and weighed, and inferences are drawn in the summary and conclusions section at the end of the text.

(U) An appendix contains a detailed account of one experiment considered by the author to be possibly quite significant.

BRIEF HISTORY OF THE AN/FPS-95

By the early 1960's, the promise that early experimenters had seen for long range, high-frequency radar apparently had been realized by the Madre OTH radar of the Naval Research Laboratory on Chesapeake Bay, when Naval Research Laboratory personnel reported detection of aircraft targets at ranges of 1,500 to 2,000 nmi (2) and of missiles in early launch phase from Cape Canaveral. (3) Plans then were made by the U.S. Air Force to incorporate this new technology into a radar sensor to be located in Turkey which, looking over the Soviet Union, Would gather intelligence data on Soviet missile and air activities, at that time the cause of much official concern.

(U) {(S)} In 1964, the U.S. Air Force solicited bids on the contract definition phase of the over-the-horizon radar in Turkey. The award was given to RCA on the basis of a design approach that closely paralleled the design of the Madre radar. In 1965, following contract definition, bids were solicited for an operational radar in Turkey, but a hiatus developed when a site in Turkey was not made available to the United States. A search for a site then was made in other countries, and after some time and negotiation, the British offered a site in Suffolk, on the coast of the North Sea near the town of Orford. The Air Force accepted this offer, and the program proceeded.

(U) {(S)} In 1966, the Air Force again solicited bids for an operational OTH radar to overlook air and missile activities in the Soviet Union and Eastern Europe, this time from England. Program management was assigned to the Electronic Systems Division of the Air Force Systems Command at Hanscom Air Force Base, Mass. Engineering responsibility before this had been assigned to the Rome Air Development Center, Griffiss Air Force Base, N.Y.; scientific support was to be furnished by the Naval Research Laboratory. Toward the end of 1966, a contract to build the radar was awarded to RCA Corp., Moorestown, N.J. The radar had by that time come to be called the AN/FPS-95 with code name Cobra Mist. In the United Kingdom, the fact that the system to be located on Orford Ness was a radar was classified at the security level of "Secret."

(U) {(S}) Construction of the radar, whose design was still heavily influenced by the Naval Research Laboratory's Madre radar, began in mid-1967. Possessing capabilities previously unrealized in either experimental or operational OTH radar, the AN/FPS-95, it soon became clear, would have to be operated initially by a crew of scientist caliber, both to verify the design concepts and to develop procedures for the ultimate RAF-USAF operational crew to use in illumination of desired regions, detection and tracking of aircraft and missile targets, extraction of signatures, and so on. In 1969, plans for the scientific program, which was called the Design Verification System Testing (DVST), were drawn by the Cobra Mist Working Group, (4) which included representatives from most of the U.S. and U.K. over-the-horizon radar groups; the DVST program was to have a duration of one year. In early 1970, The MITRE Corp., Bedford, Mass. branch and the Naval Research Laboratory were chosen to conduct the DVST program, and later in mid-1970 the Air Force formed the DVST Technical Advisory Committee to assist in the technical direction of the program.

UNCLASSIFIED

[redacted]

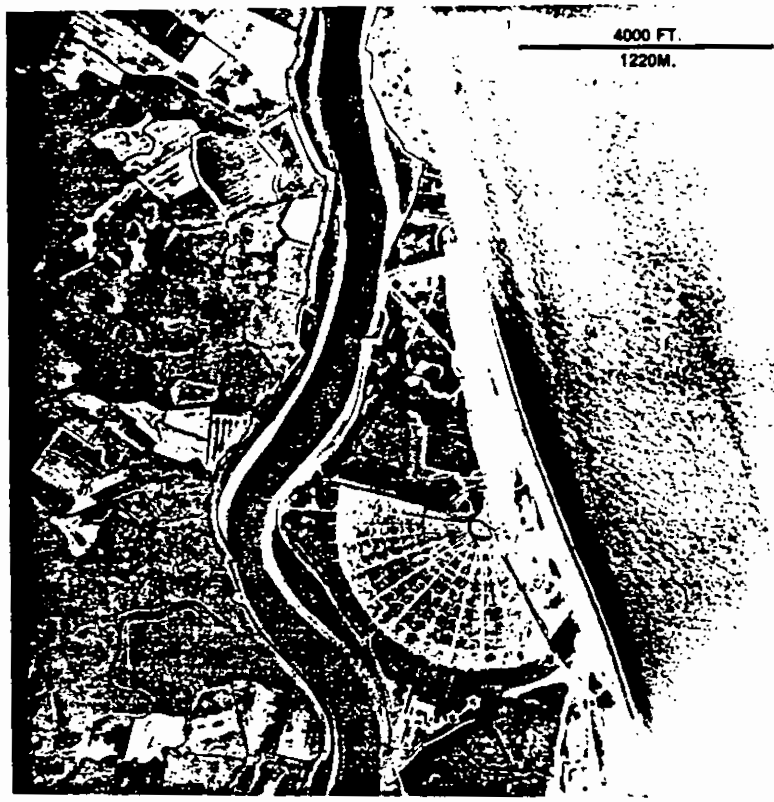

Figure 1. Aerial view of AN/FPS-95. (USAF photo.) (Figure unclassified.)

When detailed experimental plans were complete in mid-1971, groups from MITRE and the Naval Research Laboratory moved to the site, which by then had assumed the form shown in the aerial view of Fig. 1.

(U) ~~(S)~~ Technical difficulties with the system delayed both acceptance of the radar by the Air Force and the commencement of the DVST program until February 1972. From the beginning, the DVST program was hampered by problems, the most serious being the appearance of a mysterious noise which occurred in all Doppler filters corresponding to range intervals in which returns from the earth's surface (that is, "clutter" returns) were received. The range intervals containing the clutter return also contained the returns from the missile and aircraft targets the radar was to observe. The level of this "clutter-related noise" was high enough to impair seriously the capability of the radar to detect aircraft and missile targets, and as time went on, activities at the site shifted more and more from DVST to efforts to locate the source of the noise and to eliminate it.

(U) ~~(S-NF)~~ The DVST Technical Advisory Committee viewed the noise problem with increasing alarm and, in the report to the Air Force which followed its meeting in November 1972,[5] the Committee recommended that top priority be given to solving the noise problem, that control of operations at the site be shifted from the Air Force to a civilian scientific director, and that the latter mount a coordinated, systematic program to isolate and identify the source of the noise. The Air Force on Dec. 27, 1972 moved to put these recommendations into effect.

(U) ~~(S-NF)~~ DVST program was suspended, a scientific director was recruited from Stanford Research Institute, and a committee, called the Scientific Assessment Committee (SAC), was appointed with U.S. and U.K. members. The U.S. members previously had had no direct involvement with the Cobra Mist radar. This committee took a fresh look at the system, system performance, and noise data and structured a series of basic experiments[6] to determine the source of the noise. These experiments were conducted in the period from January to May in 1973, and in the ensuing appraisal it was found that the source of the noise

S[redacted]N

UNCLASSIFIED

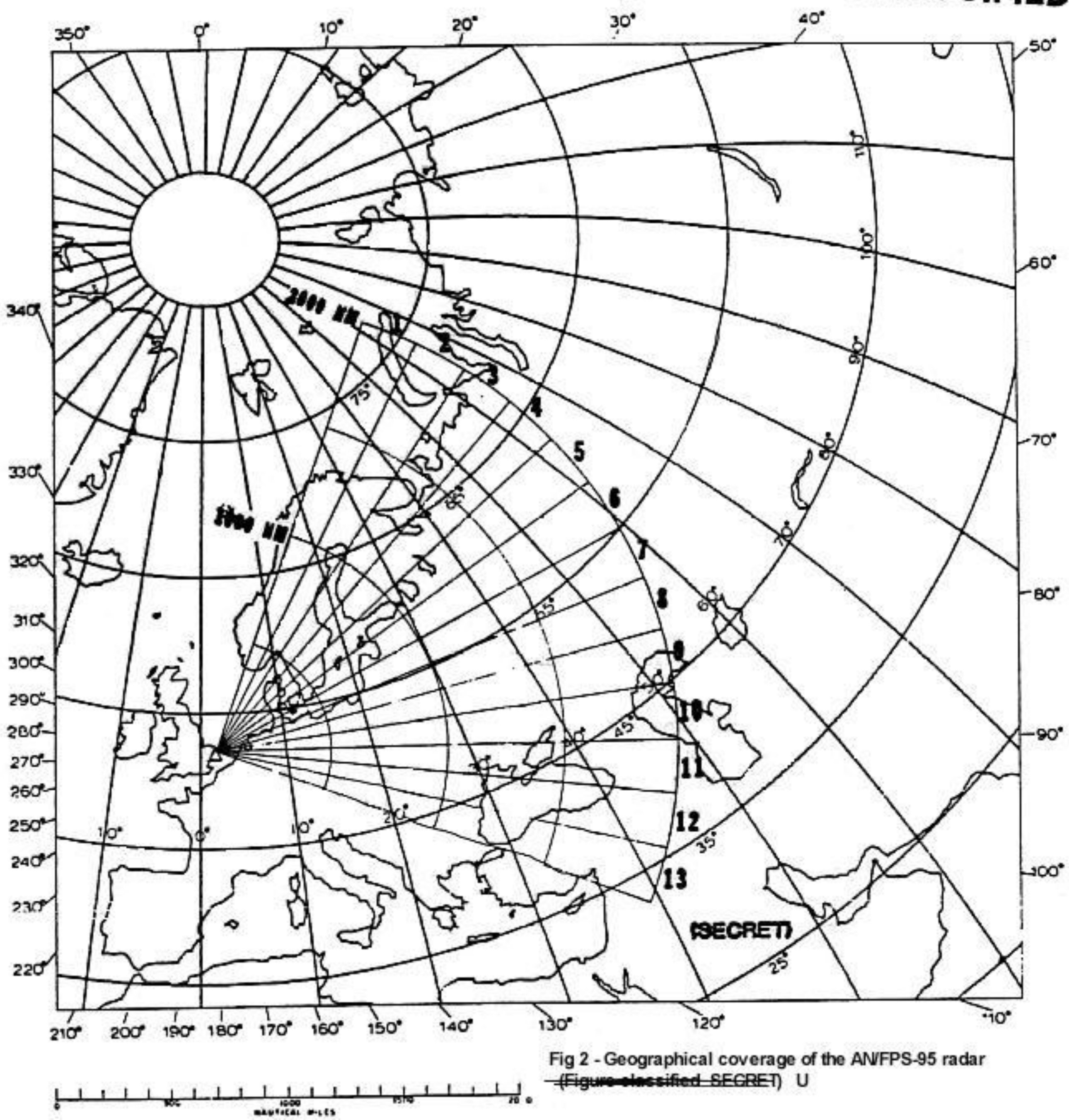

Fig 2 - Geographical coverage of the AN/FPS-95 radar
~~(Figure classified SECRET)~~ U

had not been conclusively located. The Scientific Assessment Committee submitted its report (7) in May 1973 and the Cobra Mist radar program was terminated abruptly on June 30, 1973. Afterward, the radar was dismantled, and the components were removed from the site.

(U) {(S)} So ended a program that had occupied the efforts of hundreds of people for an interval of several years and had cost the United States, by various estimates, between $100 million and $150 million. The principal product was an enigma which has not been resolved to this day.

RADAR SYSTEM DESCRIPTION

(U) ~~(S-NF)~~ The AN/FPS–95 over-the-horizon backscatter radar([8]) was located at Orford Ness on the east coast of England. By beam steering, the radar was designed to make observations within a 91–deg azimuth sector extending from 19.5 to 110.5 deg clockwise from true north. The maximum range, assuming one-hop propagation via the ionosphere F-layer, was approximately 2,000 nmi, but the equipment would permit the observation of suitable, more distant targets using multihop propagation modes. A minimum range of approximately 500 nmi was set by the lower radar frequency limit and the upper elevation limit of the radar beams. Figure 2 shows the nominal coverage of the radar using single-hop propagation modes. The operating frequency range extended from 6 to 40 MHz.

(U) The radar employed the pulse-Doppler method to detect the radar signals from moving targets against the much larger return from the earth's surface. The waveforms used for search and tracking tasks took the form of radio frequency pulses, with durations selectable from 250 to 3,000 μsec and pulse repetition frequencies (PRF) from 40 to 160 pulses/sec. Received pulse-trains of selectable lengths were processed in a frequency analyzer, which in effect provided a contiguous set of bandpass filters that were approximately "matched" in the radar sense for targets with constant Doppler frequencies and also for targets with linear Doppler rates of change (constant accelerations). An oblique ionospheric sounder mode of operation was also available, wherein the earth surface backscatter returns could be displayed as functions of radar frequency and propagation time delay.

(U) To achieve sufficient signal-to-noise ratios against the predicted noise background, the radar was capable of very high transmitted power output. A peak power of 10 MW and an average power of 600 kw were originally specified, although these figures were not achieved in practice. Such high powers were incorporated in the design to compensate for the relatively low antenna gain of approximately 25 dB.

(U) ~~(S)~~ Both ionospheric propagation limitations and the scarcity of clear HF operating frequencies impose severe limitations on the design bandwidths of OTH radar signals and therefore on the attainable range resolution. This fact, coupled with the broad (7 deg) beamwidth of the AN/FPS–95, resulted in a very large radar resolution cell and, consequently, a large earth-surface radar backscatter power. To accommodate such large signals without causing unacceptably high intermodulation and cross-modulation effects, a radar receiver with the very large linear dynamic range of 140 dB was provided, together with signal processing equipment of commensurate capabilities. A simplified block diagram of the system is shown in Fig. 3, and the major parameters are summarized in Table 1.

(U) Following are brief descriptions of the major elements of the AN/FPS–95 radar.

ANTENNA

(U) ~~(S)~~ The antenna consisted of 18 log-periodic antenna strings, which radiated like spokes in a wheel from a central "hub." Figure 4 is a close-up photograph of one such string. Each string was 2,200 ft in length and carried both horizontal and vertical radiating dipoles. The strings were separated by 7 deg in angle, and they thus occupied a 119-deg sector of a circle. The complete antenna was located over a wire-mesh ground screen, which extended beyond the strings in the propagation direction.

(U) To form a beam, six adjacent strings were connected, by means of a beam-switching matrix situated underground at the hub of the antenna, to the transmit or receive beam-forming networks in the main building. The pointing direction of the beam was controlled solely by selecting the appropriate set of six adjacent strings from among the 18 available. According to the frequency of operation, a specific small section of each log-periodic string became resonant. Thus, at high frequencies the active portion would be close to the antenna hub, and it would move out toward the larger dipole elements as the frequency was lowered. While the linear extent of the active area extending across all six strings thus increased as the frequency was lowered, the net effect was to produce a beam whose angular dimensions and, hence, gain were almost independent of frequency. A simple way to view the action of the antenna is to regard it as a six-element broadside array, which moved around within the physical boundary of

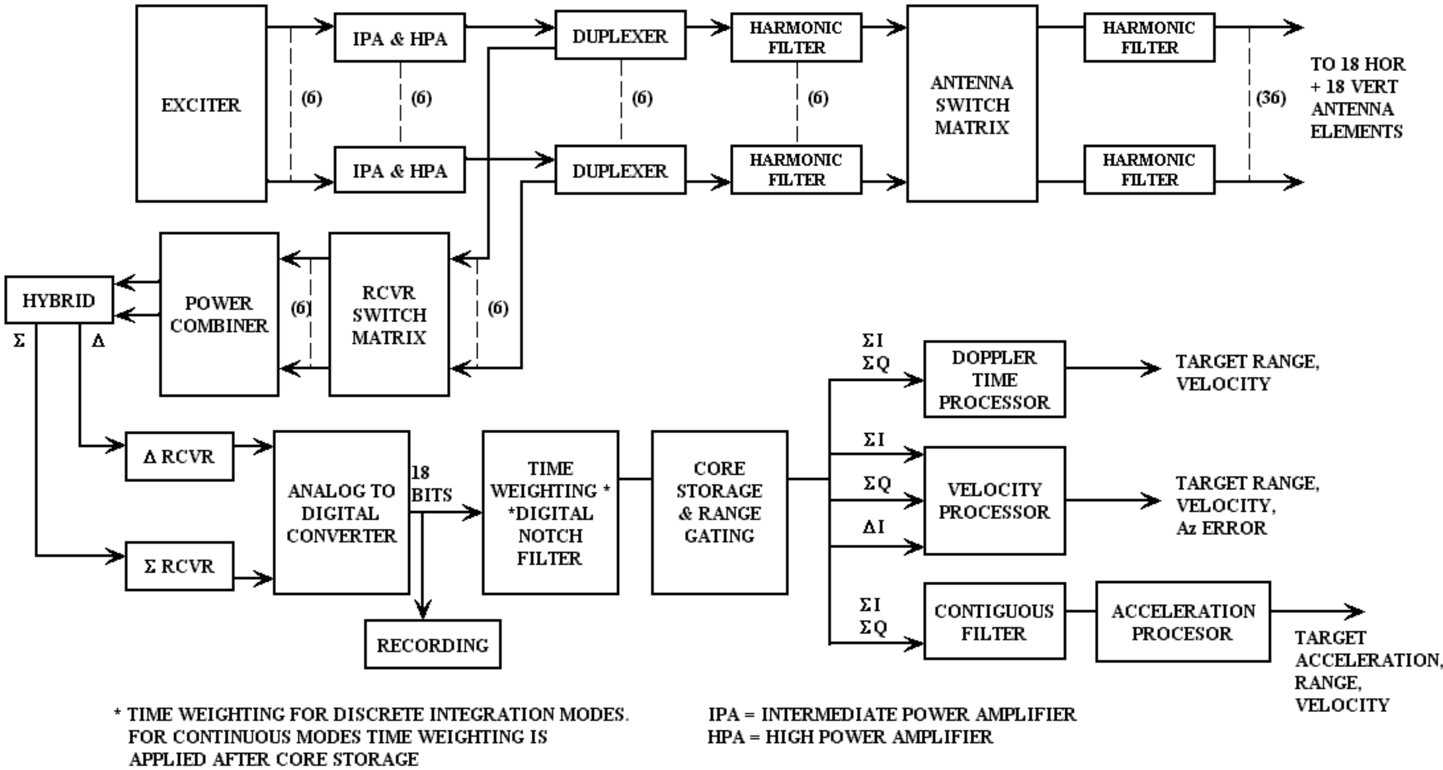

Figure 3. System block diagram (Figure unclassified.)

the antenna structure in response to frequency changes and to the choice of strings.

(U) An important point to consider is that only a small fraction of the total physical aperture of the complete antenna was devoted at any one time to the task of beam formation. To shape the beam, it was necessary to ensure that the correct phase relationships were preserved between each of the six active strings. Thus, during transmission, phase shifts were introduced in the outer four of the six strings to compensate for the arc-shaped configuration of the radiating elements and thereby produce an approximately planar wavefront. Each string was driven on transmission by a separate high-power transmitter. On reception, beam forming networks offered both in-phase addition to yield the "sum" antenna beam shape, similar to the transmission beam, and the appropriate phase shifts to yield a monopulse "difference" beam pattern for use in estimation of the target's azimuth angle.

(U) The antenna design parameters are listed in Table 2. A limited set of antenna-pattern measurements performed at the site revealed significant variations from the design values as a function of beam position and operating frequency. These variations were most pronounced in the elevation beamwidths, sidelobes, and beam-pointing directions.

TRANSMITTER-EXCITER

(U) The transmitter operated in the frequency range of 6 to 40 Mhz. Although the design called for peak powers of 10 MW and average powers of 600 kW, in practice the peek powers achieved were approximately 3.5 MW.

(U) The power was generated in six separate linear-distributed amplifiers, one of which is shown in Fig. 5. The output from each unit was fed to a separate antenna string. The power could be varied over a 20-dB range by adjusting the exciter drive level, and harmonic frequencies were filtered from the output by means of four sets of switchable low-pass filters.

(U) The exciter furnished three generic types of amplitude-modulated CW pulse shapes as follows:

TABLE 1. *AN/FPS-95 parameters.* (~~Table classified Secret.~~) (U)

Antenna	
Type	Log-Periodic Array
Frequency Range	6–40 MHz
Polarization	Vertical or Horizontal
Number of Beam Positions	13
Azimuth Coverage	91°
Azimuth Beamwidth (3 dB)	7°
Elevation Beamwidths (3 dB)	
Vertical Polarization	2° to 10°
Horizontal Polarization	9° to 30°
Gain (Vertical Polarization)	25 dB
Sidelobes	
First	-13 dB
Second	-18 dB
Other	-20 dB
Transmitter	
Type	Linear Distributed Amplifier
Frequency Range	6 to 40 MHz
Power Output	
Peak	3.5 MW
Average	300 kW
Pulse Shapes	Cosine-Squared, Flattened Cosine-Squared, Sin Mx/Sin x
Pulse Repetition Rates	10*, 40, 53.33, 80, 160 p/s
Pulse Widths	250 to 3,000 μs, 6,000 μs*
Receiver/Signal Processor	
Type	Analog and Digital
RF Bandwidth	5 kHz
Dynamic Range	140 dB
Noise Figure	7 to 14 dB (Frequency Dependent)
Analog/Digital Converter	18 Bit
Clutter Filtering	100 dB
Doppler Range	3 Hz to PRF/2
Acceleration Range	20 g
Integration Times	0.3125, 1.25, 2.5, 5, 10, 20 s

*(U) For special nonoperational use.

1. (U) Truncated $\cos^2$: This is a $\cos^2$ envelope modulation, which is truncated at the 10-percent voltage envelope points.
2. (U) Flattened $\cos^2$: This is a flat-topped pulse with truncated $\cos^2$ leading and trailing edges.
3. (U) Sin Mx/sin x: This pulse was used for the oblique ionospheric sounder mode of radar operation. The pulse was formed by the superposition of 10 carrier pulses, each of 200-μsec duration, with frequency separations of 100 kHz.

(U) The major transmitter parameters are shown in Table 3.

RECEIVER/SIGNAL PROCESSOR

(U) The receiver consisted of monopulse sum and difference channels to match the sum and difference outputs of the antenna beam-forming net-

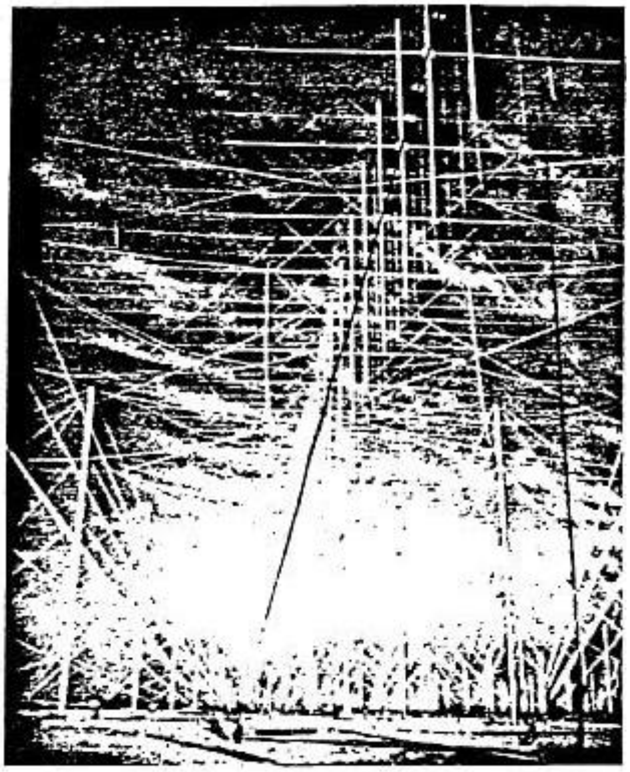

Figure 4. One of 18 log-periodic strings that formed the AN/FPS-95 radar antenna. (Figure unclassified.)

works. Each channel contained a band-switched receiver with a very large linear dynamic range (140 dB). The receiver outputs were converted to baseband frequencies by in-phase and quadrature mixers and were then converted to a digital form by means of analog-to-digital (A/D) converters.

(U) Following the analog-to-digital converters, the digital signals were time weighted to reduce the ground clutter Doppler sidelobes, digitally filtered

TABLE 2. *Antenna design parameters*. (*Table unclassified*.)

Frequency	6-40 Mhz
Gain (vertical Polarization)	25 dB
Azimuth Bandwidth (3dB)	7°
Azimuth Coverage (13 beam positions)	91°
Elevation Bandwidths (3 dB)	
Vertical Polarization	2° to 10°
Horizontal Polarization	9° to 30°
Sidelobes	-13 dB 1st sidelobe -18 dB 2nd sidelobe -20 dB other lobes

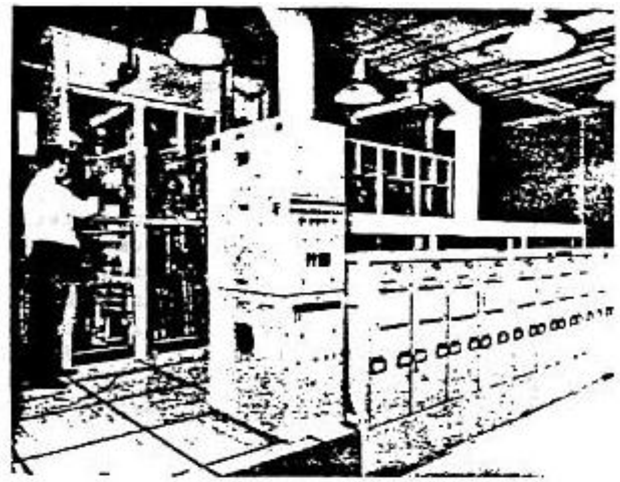

Figure 5. One of six transmitter linear amplifiers. (Courtesy RCA Corp.) (Figure unclassified.)

to remove the ground clutter, and then stored by range cell in preparation for analysis by the velocity and acceleration processors. The processing was achieved by converting the stored signal back to an analog form and then playing them back, greatly speeded up in time, with appropriate frequency translations through filters that were matched to the reconstituted pulse sequences. By these means, the entire range of Doppler shifts and acceleration profiles could be sequentially accommodated during a period shorter than that of the original radar pulse train being processed. Meanwhile, new signals were being received and stored. The durations of the pulse trains thus processed (integration times) were selectable over a range from 0.3125 to 20 sec. There was also a facility for recording the raw signals on magnetic tape at the output of the analog-to-digital con-

TABLE 3. *Transmitter parameters*

(Table unclassified.)

Frequency range	6 to 40 MHz
Power Output	3.5 MW Peak 300 kW Average
Pulse Shapes	Cos^2 Flattened Cos^2 Sin Mx/sin x
Pulse Widths	250 to 3000 microsec. 6000 microsec.*
PRF	10*, 60, 53.33, 80, 160 pulses/sec

* For special nonoperational use.

Table 4. *Receiver/signal processor parameters.* (*Table unclassified.*)

Frequency Range	6 to 40 MHz
Bandwidth	5 kHz
Dynamic Range	140 dB
Noise Figure	
6 to 15 MHz	⩽14 dB
15 to 23 MHz	⩽ 9 dB
23 to 31 MHz	⩽ 8 dB
31 to 40 MHz	⩽ 7 dB
A/D Converter	18 bit
Cluttering Filtering	100 dB
Doppler Range	3 Hz to PRF/2
Acceleration Range	20 g

verter. These data were then available for analysis off line by the extensive programs that were specially developed as part of the DVST activity or for replay through the on-line system. Some of the main receiver and signal processor parameters are listed in Table 4.

DISPLAYS

(U) The signal processor outputs contained data on target range, azimuth, velocity, acceleration, and signal amplitude. These parameters, together with a time–history dimension, could be shown on a number of cathode ray tube (CRT) displays. Intensity modulation was not employed on these displays, with the result that only two of the foregoing six parameters were displayable in the chosen x-y format at any one time. Some of the remaining parameters could be thresholded by manual selection to restrict the number of displayed data. From among all the possible combinations of the six parameters taken two at a time, the AN/FPS–95 had the capability of displaying 14 such pairs.

(U) On those displays where the signal amplitude was not one of the exhibited parameters, an amplitude threshold had to be chosen. Thus, only those signals that exceeded this threshold would be "detected" and displayed, as in a classical radar signal detection process. Cursors were provided to allow readout of parameter values from the

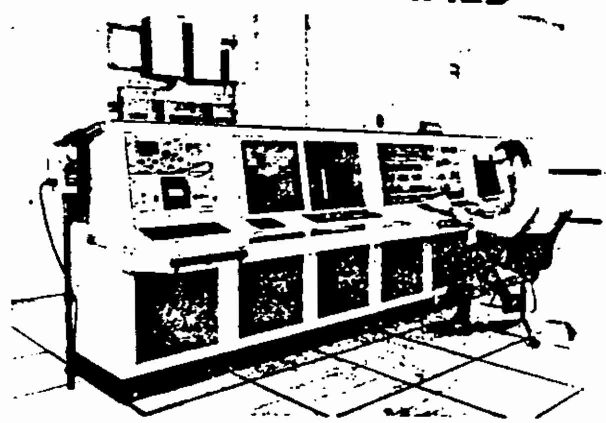

Figure 6. Radar control console. (Courtesy RCA Corp.) (Figure unclassified.)

displays, and cameras were available for a permanent display record. In addition to the presentations on the cathode ray tubes, certain data could be recorded on magnetic tape or automatically typed. Figure 6 shows a view of the radar control console with its associated displays.

ANCILLARY EQUIPMENT

(U) To support the AN/FPS–95 operation in the selection of radar operating frequencies, the site contained a vertical ionospheric sounder and a panoramic radio receiver.

RADAR CAPABILITIES AND LIMITATIONS

EXPECTED CAPABILITIES

(U) ~~(S)~~ The AN/FPS–95 was expected to detect and track (*a*) aircraft in flight over the western part of the Soviet Union and the Warsaw Pact countries and (*b*) missile launches from the Northern Fleet Missile Test Center at Plesetsk. Aircraft detection and tracking at ranges of 500 to 2,000 nmi, corresponding to one-hop ionospheric propagation, were considered feasible. Missile launches from Plesetsk were also within one-hop range from the radar. A searchlight mode was provided for high-priority targets whose approximate locations were known a priori. These targets could be single aircraft, compact formations of aircraft, or missile launches. In this mode, the radar continuously illuminated a small geographical area to obtain the maximum data rate on the selected targets. As an alternative, a scanning mode was provided, which allowed the radar to search in azimuth and range over any chosen sector of the radar coverage at a reduced data rate for any particular area. Scanning in azimuth was implemented by switching the antenna among the 13 discrete beam positions. Range-scanning was implemented by two methods: (*a*) switching between the lower and upper elevation beams and (*b*) varying the transmitted frequency as required by ionospheric propagation conditions to reach the desired range. Frequency selection was facilitated by an oblique sounding mode of the radar and by a separate vertical sounder. The scanning mode was intended for detection of targets whose locations were unknown a priori and for time-sharing the radar among different missions.

(U) {(S)} Both accuracy and resolution of the AN/FPS-95 were expected to be considerably lower than for a typical Picowave search radar. The azimuth beamwidth of 7 deg determined the angular resolution. Monopulse beam-splitting provided a nominal 1-deg angular accuracy, but this was further limited by ionospheric tilts, which could amount to several degrees, particularly in the northern beams that approached the auroral region. The unmodulated radar pulses provided only coarse range resolution. With the longest pulse, 3 milliseconds in duration, the range resolution equaled 240 nmi. The shortest pulse, 250 microseconds., provided a nominal 20-nmi range resolution, but this pulse could be used only under a limited number of conditions. Pulse-splitting in range could be performed manually on the displays to obtain a slant range accuracy of perhaps one-third of the range resolution, but the accuracy with which slant range could be converted to ground range was limited by uncertainties in virtual height of the ionosphere.

(U) Against this coarse spatial accuracy and resolution was set the fine Doppler resolution of the radar. Coherent integration times of 10 sec were frequently allowed by the ionospheric propagation medium, providing a range-rate resolution of 1.5 knots at the midband frequency of 20 MHz. The fine Doppler resolution was intended both for separation of multiple targets and for discriminating moving target returns from stationary ground backscatter.

(U) The expected capability of the AN/FPS-95 were based primarily upon experience with the Madre OTH-B radar constructed in Maryland by the Naval Research laboratory. Aircraft detection and tracking over the North Atlantic was reported by Madre experimenters at one-hop ranges on several occasions. (2) Missiles launched from Cape Canaveral were also said to have been detected. (3) Since the AN/FPS-95, like Madre, was a monostatic pulse Doppler HF radar with high transmitter power, coarse spatial resolution, and fine Doppler resolution, its detection and tracking performance was expected to be roughly similar. The siting of the AN/FPS-95 provided two operational differences between it and Madre, however: (*a*) Interference in the HF band was worse in Europe, particularly at night, and (*b*) ground backscatter was usually received by the AN/FPS-95, rather than sea backscatter.

(U) {(S)} Performance of the AN/FPS-95 was projected (9) using the ITS-78 ionospheric propagation prediction computer program, (10) as modified by MITRE personnel for radar use. This program was designed to support long-range HF communications, and its utility for predicting OTH-B radar performance, a more demanding application, was not established. Nevertheless, it was the best tool available at the time and was therefore used. Single-dwell probability of detection for aircraft was estimated for a representative assortment of target areas, and it appeared adequate for a searchlight mode with repeated dwells in a given geographical area, but marginal for a scanning mode having a low data rate on any particular target.

(U) {(S)} It was also recognized at the time that ground backscatter would be orders of magnitude larger than aircraft returns or missile skin returns. Ground backscatter cross section Xs, is given by

$$Xs = 1/2\ Xu\ R\ Tb\ C\ r\ \sec Ai \qquad (1)$$

Take typical values of the parameters for an example. Setting backscattering cross section per unit area Xu equal 0.02 (-17 dB), range R equal 1,350 nmi, azimuth beamwidth Tb equal 7 deg, pulse length r equal 1 msec, and angle of incidence Ai equal 8 deg, gives Xs, equal to $1.06 \times 10^9\ m^2$ (90.2 dBSM). Given a typical aircraft radar cross section Xt of 30 m^2 (14.8 dBSM) at HF, the ratio Xt/Xs, equals -75.4 dB. In order to achieve a 10- to 15-dB signal-to-clutter ratio for high single-dwell probability of detection in a scanning mode, the pulse Doppler radar signal processor was required to suppress the ground backscatter by 85 to 90 dB relative to aircraft returns—that is, to provide 85 to 90 dB of subclutter visibility (SCV). Somewhat lower probability of detection, and hence less subclutter visibility, would suffice for the searchlight mode, where the radar continuously illuminated a given target. In an attempt to achieve the required subclutter visibility, great care was taken in the design of the radar transmitter to minimize spectral noise and in the receiver and signal processor to minimize intermodulations and cross modulations and to provide a large linear dynamic range.

DESIGN VERIFICATION SYSTEM TESTING (DVST)

(U) ~~(S)~~ Following construction of the AN/FPS-95 and its acceptance by the government, a one-year research and development program was planned[4] to assess its capabilities. The 12 aircraft detection and tracking experiments assigned to MITRE during the DVST will be described briefly as a further indication of the expected capability of the radar. A number of other experiments, including all of the missile detection and tracking experiments, were assigned to Naval Research Laboratory and have been documented by that organization.[11] This paper will therefore discuss only aircraft detection and tracking, with which the authors have firsthand experience.

(U) ~~(S)~~ Experiment 202, Radar Aurora, was intended to determine experimentally the effects of HF radio aurora on OTH radar design and operation. Experiment 104, Signal Detectability, and Experiment 502, Target Detection and Calibration, were to determine probability of detection, probability of false alarm, and signal-to-noise ratios of detected targets, as well as develop procedures to estimate radar cross section of the detected targets. Three experiments dealt with real-time tracking of aircraft at the radar consoles and were designed to develop and evaluate this capability: Experiment 501, Evaluation of Target Window Printout; Experiment 505, Tracking Through Azimuth Beams; and Experiment 508, Track Capability and Track Sample Rate. One experiment dealt with automatic tracking of aircraft, conducted off line on a digital computer. This was Experiment 405, Track-While-Scan Feasibility. Experiment 506, Range and Azimuth Calibration, was intended to provide an absolute spatial calibration using ground transponders.

(U) ~~(S)~~ These eight experiments were intended to assess the general capabilities of the radar for aircraft detection. Four other experiments were directed toward specific intelligence objectives. Experiment 306, Vertical Velocity Estimation with Aircraft, was to exploit the fine Doppler resolution of the radar to measure vertical velocity. The Doppler difference between alternate ground-reflected propagation modes was to be utilized for this purpose. Experiment 312, Intelligence from Test Range Calibration Flights, surveyed aircraft activity near Plesetsk and other missile test centers. Experiment 314, Reconnaissance Aircraft Surveillance, tracked friendly aircraft over the Baltic Sea area, providing the only source of over-water aircraft tracking data. Experiment 315A, Aircraft R&D Test Intelligence, observed aircraft at the Ramenskoye and Vladimirovks Flight Test Centers.

(U) Of these 12 experiments, three were carried out and documented: Experiments 202,[12] 405,[13] and 506.[14] The rest were not completed for either of two reasons: (*a*) The experiment as conceived proved too ambitious for the actual capability of the radar or (*b*) the scientist assigned to the experiment was reassigned to efforts to improve the radar capability.

OBSERVED CAPABILITIES AND LIMITATIONS

(U) ~~(S)~~ Once DVST got under way at Orford Ness, it became apparent to the MITRE team (and others) on site that the actual radar capabilities were a good deal less than the expected capabilities. In the searchlight mode, aircraft detection and tracking were marginal, even when aircraft flight plans were known a priori. When the radar was carefully operated, with due regard for range and Doppler ambiguities and ionospheric propagation conditions, tracking trials on known aircraft in the searchlight mode produced tracks less than half the time. Furthermore, the tracks obtained were discontinuous, the aircraft return usually being above the noise level only near the peaks of the Faraday rotation and multipath fading cycles. Additionally, routine observations of areas of high air-traffic density, such as air routes near Moscow, in the searchlight mode often produced few or no target detections at times of day when the propagation was good and the aircraft density in the illuminated area was known to be high.

(U) {(S)} Capability in a scanning mode was essentially nonexistent, because of both the unexpectedly low signal-to-noise ratio on aircraft returns and the difficulty of making appropriate frequency selections for the large number of scan positions. In practice, the poor performance in the searchlight mode discouraged the experimenters from making much use of the more ambitious scanning mode.

(U) {(S)} Some general observations during aircraft detection and tracking are worth recording, in light of the later discussion on the physical phenomena limiting radar performance.

1. (U) {(S)} Daytime performance was much better than nighttime performance. This was unexpected, because D-region absorption is much higher during the day than at night. Such diurnal variation in performance is the opposite of long-range HF communications experience.

2. (U) {(S)} Aircraft could be detected and tracked over the Baltic Sea better than over land in most cases.

3. (U) {(S)} Aircraft detectability was not maximized at the angle of maximum ground backscatter, but rather at a somewhat greater range, often near the trailing edge of the ground backscatter. It was surmised that aircraft returns fell off with range more slowly than ground backscatter, since the radar cross section (RCS) of aircraft Xt, is independent of range, whereas Xs increases as grazing incidence is approached; that is, Xo increases much faster than R increases in Eq. (1).

4. (U) {(S)} Shorter pulses and higher PRF's generally provided more aircraft detections than longer pulses and lower PRF's. This observation is consistent with a clutter-limited radar whose subclutter visibility increases with Doppler shift.

(U) {(S)} As experience was gained with the AN/FPS-95, the factors limiting radar performance became clear. These were clear channel availability, a lack of radio frequencies below 6 MHZ, the two-level radar displays, and (worst of all) the limited subclutter visibility. A clear channel is a 5-kHz frequency band in which no significant interference exists; that is, the noise power spectral density approximates the atmospheric and galactic noise predictions of CCIR Report 322 (15) or the rural man-made noise model of the ITS-78 report, (10) whichever is larger. In the searchlight mode, one could take a few minutes to look carefully for a clear channel, but this was not possible for the scanning mode. During the day, clear channels were generally available at Orford Ness, particularly, for illuminating the longer one-hop ranges with radio frequencies above 20 MHz. Clear channels were less often available at night, when radio frequencies from 6 to 8 MHz were required. The large number of HF radio stations in Europe all operated in the same frequency region at night, Particularly the 41-meter and 49-meter international shortwave bands. The fact that the radar could not operate below 6 MHZ also limited performance at night, since the maximum usable frequency (MUF) for the shorter one-hop ranges was sometimes below 6 MHz. The shorter ranges could not be illuminated by the radar when this occurred.

(U) {(S)} The radar displays were also a significant limitation of real-time aircraft detection and tracking. The Doppler-time and Doppler-range displays had only two intensity levels - on and off. The lack of a gray scale to show a dynamic range of signal and noise amplitudes made target detection difficult. Setting the on/off amplitude threshold appropriately for fading targets in a fluctuating noise level that varied from range bin to range bin was a challenging task. Better target detection and tracking were obtained offline with computer generated displays having an amplitude scale, some of which are illustrated later in the paper. An improved online radar display was developed (16) and brought to the AN/FPS-95 site just before the radar was shut down. While this had only a very brief trial, it did show promise of considerably improved detection and tracking capability compared to the radar displays.

(U) {(S)} The most important constraint on radar performance was the limited subclutter visibility. Instead of a projected 85- to 90-dB subclutter visibility, the radar was found to have only 60- to 70-dB subclutter visibility. Target detectability was degraded by a noiselike clutter residue which often could be 20 dB, and in some cases even 30 dB, higher than the level of external noise received by the radar. Figure 7 is a photograph of the AN/FPS–95 Doppler-range display taken early in the DVST.(17) The range scale (horizontal) extends from 0 to 2,000 nmi, the nominal unambiguous range at a PRF of 40 HZ. The Doppler scale (vertical) extends from 3 to 20 HZ, with approaching and receding Doppler shifts folded together. A Doppler shift of 20 HZ corresponds to a radial velocity of 264 knots at the radio frequency of 22.1 MHZ employed to obtain these data. Ground backscatter in the 0- to 3-HZ region is suppressed by the digital clutter filter. In some range bins, corresponding to the skip zone for ionospheric propagation, the noise level is below the display threshold in all Doppler bins. In the succeeding range bins, generally corresponding to the ranges of first-hop ground backscatter, the noise level in all Doppler bins is much higher, hindering target detection.

(U) ~~(S)~~ That the excess noise seen on the radar displays was in fact clutter-related was demonstrated clearly by turning off the radar transmitters. This caused the display of Fig. 7 to go black. When the threshold was readjusted to observe the noise level, it was observed to be constant with range, as one would expect from external noise. After a number of such observations, it became apparent that even if a clear channel could be found, even if ionospheric propagation to the desired geographical area existed at the clear channel frequency, and even if the radar display limitations could be overcome, the excess noise would still provide a severe limitation on radar performance. Therefore, in parallel with DVST, an effort to characterize the excess noise was undertaken on site.

CHARACTERISTICS OF THE EXCESS NOISE

(U) ~~(S)~~ The radar displays presented the excess noise in a dramatic way, but a quantitative characterization of the phenomenon required the use of off-line digital signal processing programs.(18) The output of one of these programs is illustrated in Fig. 8 for data recorded near 7:00 Greenwich mean time on March 4, 1972 (Day 64) in beam 11 with vertical polarization at 22.1 MHZ—the same data as previously illustrated in Fig. 7. The variation of ground backscatter (clutter) and excess noise amplitude with slant range is plotted in Fig. 8.

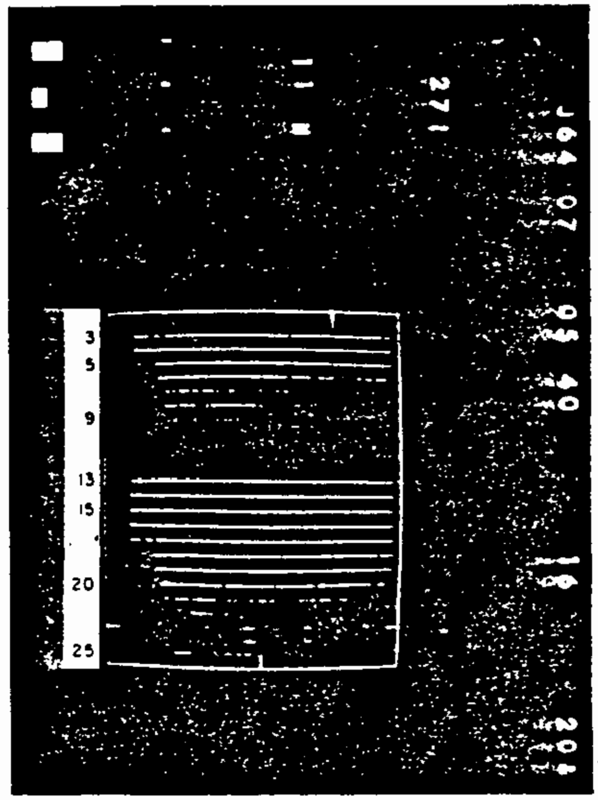

Figure 7. Doppler/range display illustrating excess noise (Figure unclassified.)

Note that the clutter curve is moved downward by 50 dB to facilitate comparison with the noise curve. Ground-clutter amplitude was computed by peak selection in a ±1.5-HZ Doppler window. The amplitude of excess noise was computed by averaging the squared modulus of the digital signal processor output over all Doppler bins from 3 to 20 HZ on either side of the carrier, that is, over all those Doppler bins outside the radar clutter filter rejection band. The digital signal processor performed a fast Fourier transform (FFT) over 512 successive radar pulses in each 12.8-sec coherent integration interval. The plotted clutter and noise powers were then further noncoherently averaged over 15 successive coherent integration intervals.

(U) ~~(S)~~ One sees in Fig. 8 a marked variation of the excess noise amplitude with slant range. Strong excess noise exists at short range, in the skip zone just ahead of the ground clutter, and at the range of the ground clutter. The excess noise near the range of peak ground backscatter varies with range in direct proportion to the backscatter,

296-318 O - 79 - 2

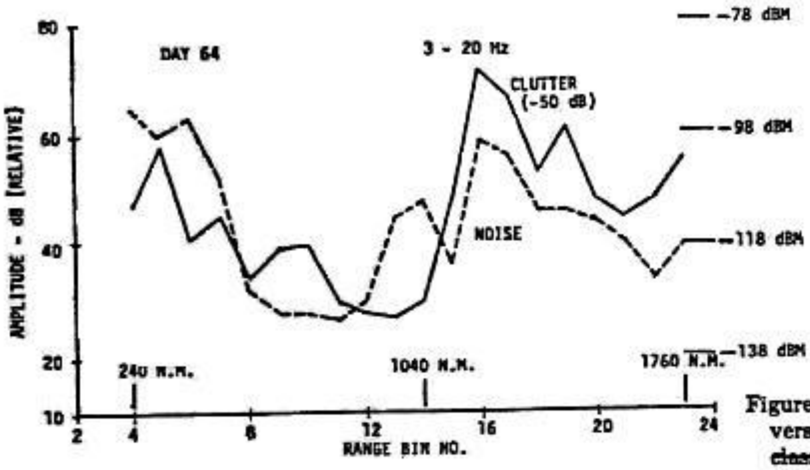

Figure 8. Clutter and noise amplitude versus slant range.[17] (~~Figure classified Secret.~~) (U)

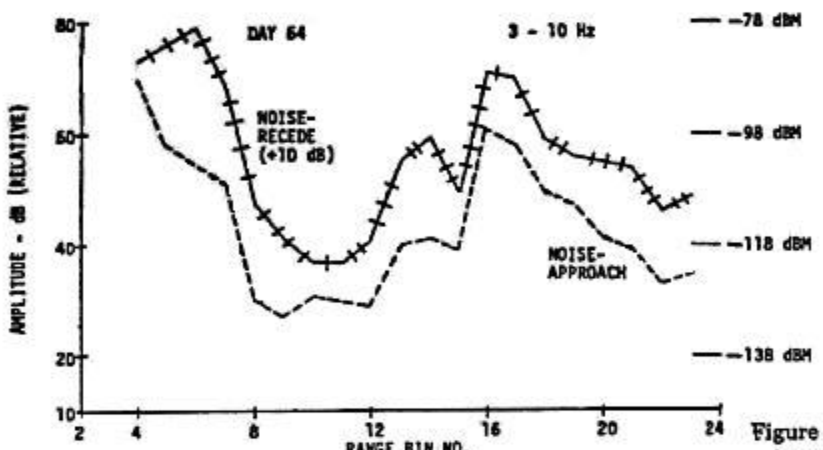

Figure 9. Approach/recede difference in noise amplitude.[17] (~~Figure classified Secret.~~) (U)

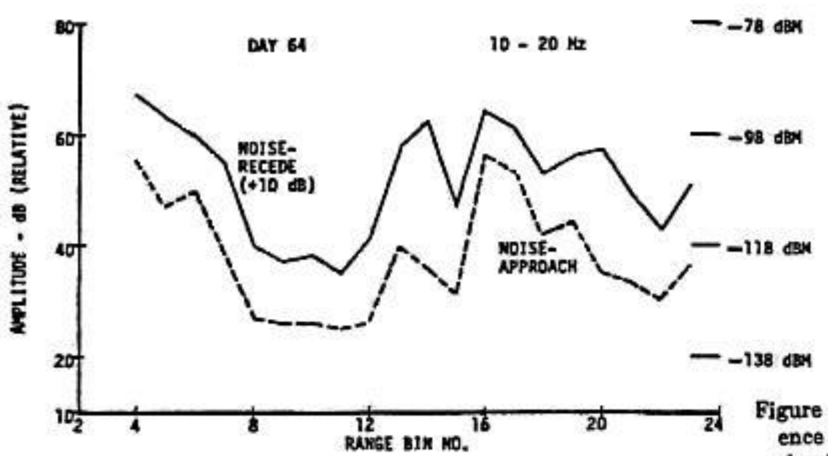

Figure 10. Approach/recede difference in noise amplitude.[17] (~~Figure classified Secret.~~) (U)

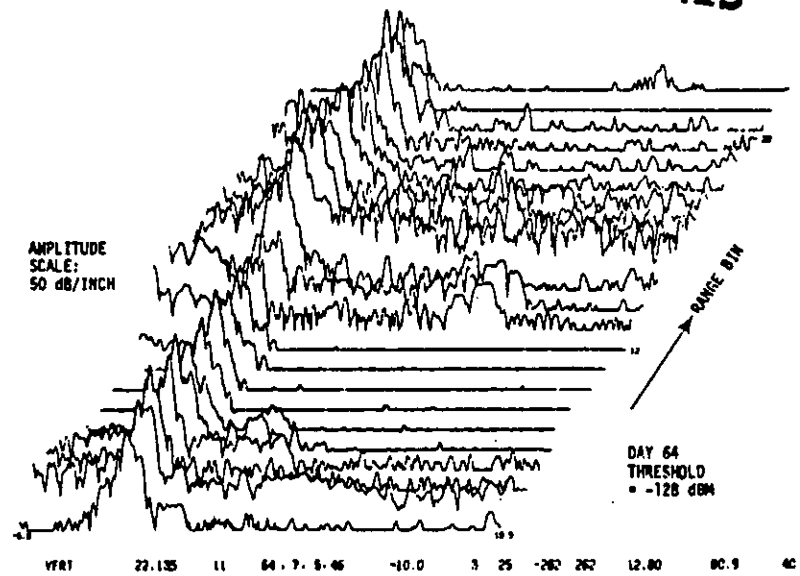

Figure 11. Range/Doppler display of excess noise.[17] (~~Figure classified Secret.~~) (U)

but the excess noise at short range and in the skip zone does not. To distinguish between the excess noise that occurs ahead of the ground clutter and the excess noise that occurs at the range of ground clutter, special terminology was used at the site. All sources of excess noise that varied with range were termed "range-related noise" (RRN). The portion of the excess noise that coincided in range with ground clutter was termed "clutter-related noise" (CRN). Although all of the range-related noise was of scientific interest, only the clutter-related noise interfered with detection of aircraft, which was the primary mission of the radar. To better characterize range-related noise, Figs. 9 and 10 were generated from the same data.[17] Here, the average power of range-related noise is computed separately for approaching and receding Doppler bins. In Fig. 9, noise power is averaged over Doppler bins 3 to 10 Hz from the carrier, while in Fig. 10 noise power is averaged over Doppler bins 10 to 20 Hz from the carrier. One sees that the clutter-related noise near the range of peak ground backscatter has a symmetrical spectrum close in (3 to 10 Hz) and a nearly

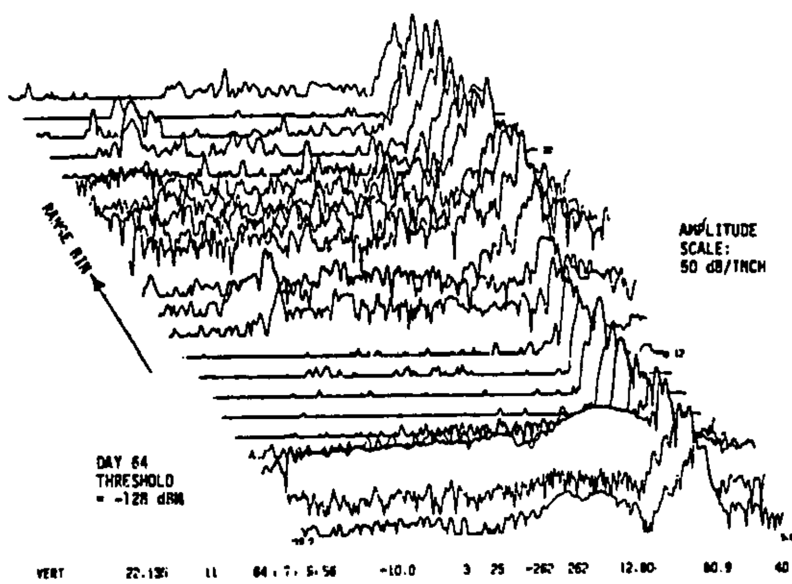

Figure 12. Range/Doppler display of excess noise.[17] (~~Figure classified Secret.~~) (U)

UNCLASSIFIED

S[redacted]

Figure 13. Doppler/time display of excess noise.(17) (~~Figure classified Secret.~~) (U)

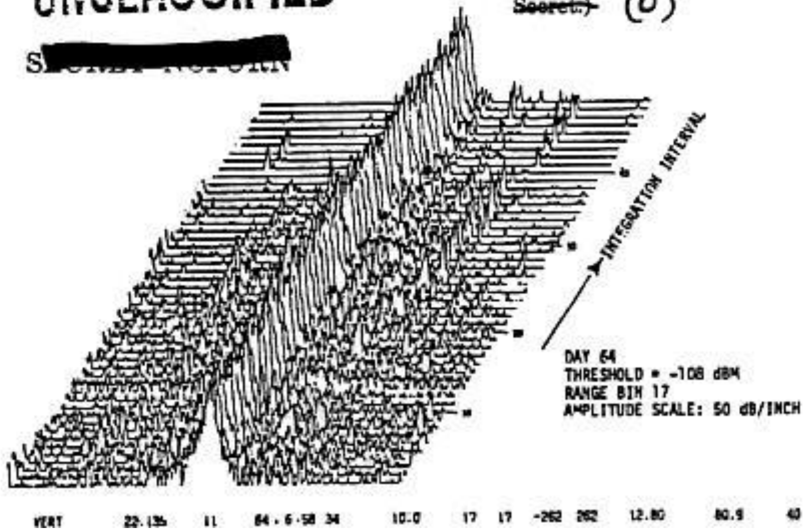

symmetrical spectrum farther out (10 to 20 HZ). The range-related noise in the skip zone, on the other hand, has considerably more power in receding Doppler bins than in approaching Doppler bins. So does the range-related noise at short range, particularly from the 3- to 10-HZ Doppler bins. By comparing Figs. 9 and 10, one sees that range-related noise does decrease with increasing Doppler shift, although the true spectral extent of the range-related noise is obscured by the spectral replication that occurs at the radar PRF of 40 Hz.

(U) {(S)} A more graphic, if less quantitative, presentation of the computer-processed data is given in Figs. 11 and 12. (17) Amplitude versus frequency (Doppler) is plotted over a +- 20-Hz band for successive 80-nmi radar-range bins during one particular 12.8-sec coherent integration interval. Figure 11 shows the approaching Doppler bins, while Fig. 12 shows the receding Doppler bins. This presentation shows the variation of range related noise with range and Doppler quite clearly. To show the temporal fluctuation in noise level, as well as the spectral rolloff, Fig. 13 shows amplitude versus Doppler during successive coherent integration intervals, for radar-range bin 17, which is at 1,280-nmi slant range, near the peak of the ground backscatter. The data in Figs. 11, 12, and 13 are thresholded, which has been found to produce a more easily interpreted display. The

Figure 14. Doppler/time display of excess noise.(17) (~~Figure classified Secret.~~) (U)

S[redacted]

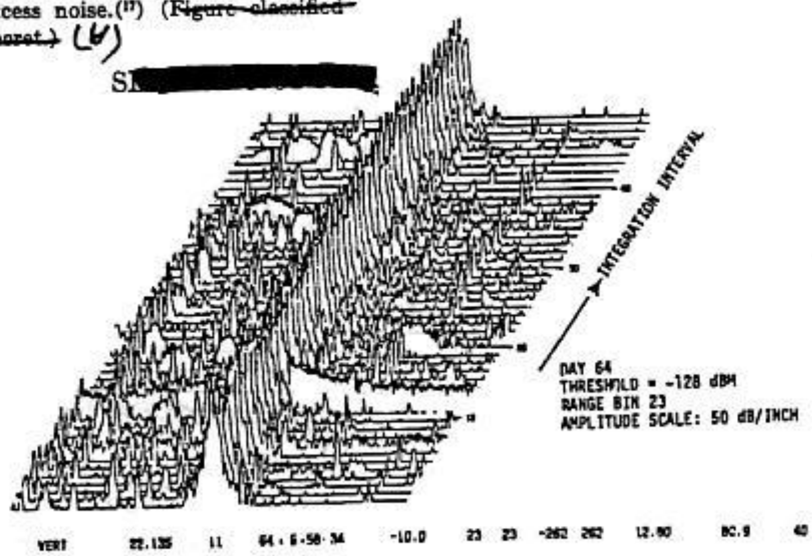

UNCLASSIFIED

threshold for Fig. 13 is 20 dB higher than the thresholds of Figs. 11 and 12 to show the clutter-related noise peaks more clearly.

(U) ~~(S)~~ Figure 14 shows amplitude versus Doppler during successive coherent integration intervals for radar-range bin 23, which is 480 nmi behind the peak of the ground backscatter, but still illuminated by one-hop ionospheric refraction.[17] In particular, this range bin, at a slant range of 1,760 nmi, represents a ray path elevation of only a few degrees at ground level for one-hop propagation by means of the F2 layer of the ionosphere. The amplitude of range-related noise is much lower in range bin 23 than in range bin 17, which can be seen by noting that Fig. 14 has a threshold 20 dB lower than that of Fig. 13. One also notes in Fig. 14 a number of possible aircraft tracks (large amplitude returns isolated in Doppler and forming a Doppler–time trace) from the geographical area illuminated, which contained a number of Soviet military airfields. All of these apparent target returns in range bin 23 are well below the level of clutter-related noise seen in range bin 17. Thus, if the targets were in range bin 17, 480 nmi closer to the radar, they probably would not have been detected, even allowing for a 5.5-dB greater radar return due to the decreased range. Figure 14 illustrates the contention made earlier that aircraft detectability was not maximized at the range of peak ground backscatter, but rather at somewhat greater ranges, where grazing incidence for ground backscatter was approached.

(U) ~~(S)~~ The radar data illustrated, taken on a single day early in the DVST period, are reasonably representative of the range-related noise phenomenon. Characteristics of range-related noise observed throughout the period of AN/FPS–95 operation are summarized here:

(U) *1.* ~~(S)~~ Range-related noise was observed predominantly at three positions: at short range, in the skip zone ahead of the ground backscatter, and at the ranges of ground backscatter.

(U) *2.* ~~(S)~~ Both components of range-related noise at shorter ranges than ground backscatter had asymmetrical frequency spectra, with more power in receding Doppler than in approaching Doppler. The clutter-related noise at the ranges of ground backscatter generally had a more symmetrical frequency spectrum. Range-related noise decreased slowly with increasing Doppler shift in all three cases.

(U) *3.* ~~(S)~~ The amplitude ratio of ground backscatter to clutter-related noise near the range of peak ground backscatter (where the radar was intended to detect targets) was relatively constant, being in the range of 60 to 70 dB.

(U) *4.* ~~(S)~~ The amplitude ratio between range-related noise and external noise (noise received with the transmitter off) was more variable, depending on both the absolute level of ground backscatter and the level of external noise. Ratios varying from 10 to 30 dB were typical. The only times range-related noise exceeded external noise by less than 10 dB were the times when geographical areas of interest were weakly illuminated or the external noise level was very high. These were times, of course, when the radar would have had little detection and tracking capability, even in the absence of clutter-related noise.

(U) *5.* ~~(S)~~ Range-related noise was observed to occur at all times of the day, in all seasons, in all beams, at all radio frequencies, in both polarizations, and so on. It was not an isolated phenomenon.

THE SEARCH FOR SOURCES OF EXCESS NOISE IN THE RADAR

(U) ~~(S)~~ Once the effects of clutter-related noise on radar performance were understood, the AN/FPS–95 underwent extensive testing to see if the clutter-related noise might be originating in the equipment itself. There were two motives for first testing the radar itself before carrying the investigation to possible external causes of clutter-related noise:

(U) *1.* ~~(S)~~ Before using the radar as a test instrument to look for causes of clutter-related noise in the ionospheric propagation medium or in reflection phenomena in the target space, it was necessary to verify that the radar itself was not the principal cause of the observed clutter-related noise.

(U) *2.* ~~(S)~~ It was thought that, if sources of clutter-related noise could be located in the radar equipment, they could probably be alleviated by repair or modification of the offending components. If, on the other hand, sources of clutter-related noise were found in the propagation medium or in the target space, little could be done to improve radar performance short of extensive redesign of the radar for better spatial resolution.

(U) {(S)} The results of this extensive radar testing are described here. First is a concise account of each of the principal tests conducted. The tests are grouped according to the radar component tested, rather than chronologically. Second, the main equipment-related, hypothesized causes of clutter related noise are listed and compared with the test results by means of a matrix. Third, the overall conclusions of the radar testing are given, namely, that the radar hardware was not the principal cause of clutter-related noise.

EQUIPMENT TESTS FOR CLUTTER-RELATED NOISE

(U) {(S)} The equipment test descriptions, while not a complete account of all tests conducted on site, represent most of the tests for which documentation is available, and we believe they give a reasonably comprehensive picture of the radar's capabilities. Tests of the radar transmitting chain are described first. The objective of these tests was to measure spectral noise on the transmitted signal, to see if it was comparable in amplitude to the levels of clutter-related noise observed on ground clutter.

Test 1: Transmitter Noise Level (19)

- (U) *Description:* Measure spectral noise level of HPA #4 at 10 and 30 Hz from carrier frequency.
- (U) *Results:* Noise level was 98 to 102 dB below carrier at 10 HZ and 102 to107 dB below at 30 HZ.
- (U) *Frequencies:* 7, 13, 18, and 27 MHZ.
- (U) *Dates:* January and February 1973.

Test 2: Fan Dipole on Sea Wall #1 (20)

- (U) *Description:* Transmit at high power from one or more strings of the radar antenna. Connect vertically polarized fan dipole to radar receiver and signal processor and measure spectral noise level.
- (U) *Results:* Noise level was down 80 to 100 dB with radar antennas vertically polarized at all frequencies. With radar antenna horizontally polarized, noise level was down only 37 dB in 10- to 15-MHz frequency band, but down 70 to 85 dB at frequencies above 17.5 MHz. Spectral noise was linear with transmitter power.
- (U) *Frequencies:* Various.
- (U) *Date:* Oct. 30, 1972.

Test 3: Fan Dipole on Sea Wall #2 (21)

- (U) *Description:* Transmit at full power from five strings of beam 13. Connect fan dipole to receiver and signal processor and measure noise level.
- (U) *Results:* Spectral noise down 91 to 94 dB with both radar antenna and fan dipole vertically polarized.
- (U) *Frequency:* 20.67 MHZ.
- (U) *Dates:* Unknown.

(U) {(S)} A number of receiving chains tests are now described, each directed toward a possible cause of clutter-related noise. The objective of these tests was to determine the linear dynamic range of the radar receiver end other components in the receiving chain, to see if the observed clutter related noise could be originating in the receiving chain. The general approach was to inject test signals of high spectral purity at various points in the receive chain and to measure the resulting spectral noise at various output points.

Test 4: Receiver Linear Dynamic Range (19)

- (U) *Description:* Input-output testing of receiver was performed to measure selectivity, noise figure, linearity, and dynamic range.
- (U) *Results:* Receiver performance was close to design goals. Spurious-free dynamic range was 111 to 122 dB.
- (U) *Frequencies:* All receiver bands, 6 to 40 MHZ.
- (U) *Dates:* January and February 1973

Test 5: Receiver Intermodulation (22)

- (U) *Description:* Measure in-band intermodulation (IM) levels at several frequencies.
- (U) *Results:* In the 6- to 15-MHz band, the fifth order intermodulation product was down 74 to 77 dB for -18 dBM in-band input signal; the ninth-order intermodulotion product was down 82 to 85 dB. These were worst cases, since (*a*) most intermodulation products were considerably lower, and (*b*) a -18 dBM input signal is much larger than average.
- (U) *Frequencies:* 7, 8, 9, 12, 16, 19, 20, and 35 MHz.
- (U) *Dates:* Feb. 14, Feb. 16, and March 23, 1972.

Test 6: Receiver and Duplexer Cross Modulation (CM) (23)

- (U) *Description:* Inject two test signals 10 HZ apart at 1 MHZ from the desired signal. Measure the cross modulation level on the desired signal.
- (U) *Results:* The cross modulation level was 82 to 85 dB down from the desired signal for a −10 dBm out-of-band input, in the worst case. Duplexer cross modulation effects were negligible.
- (U) *Frequencies:* 8 and 16 MHZ.
- (U) *Dates:* April 22 and April 28, 1972.

Test 7: Radio-Frequency Hardware Measurements(19)

- (U) *Description:* Measure spurious-free dynamic range of transmit/receive diodes and magnetic elements in the beam-forming network.
- (U) *Results:* No degradation in subclutter visibility by these components was found, unless electromagnetic interference (EMI) approaches 0 dBm, which is rare.
- (U) *Frequencies:* Not given.
- (U) *Dates:* January and February 1973.

Test 8: Electromagnetic Interference Measurements(24)

- (U) *Description:* Measure the power level of interfering HF signals at the receiver input, mostly in beam 7 with horizontal polarization.
- (U) *Results:* Out-of-band electromagnetic interference sometimes exceeded receiver ratings below 15 MHZ. Out-of-band electromagnetic interference seldom exceeded receiver ratings above 15 MHZ.
- (U) *Frequencies:* 5 to 10, 10 to 15, 15 to 20, and 20 to 25 MHZ.
- (U) *Dates:* Dec. 28 through 30, 1971.

Test 9: Simulated Clutter into Receiver(25)

- (U) *Description:* Inject a simulated clutter signal into the receiver at a range in the skip zone, ahead of actual ground clutter received in beams 1, 7, and 13 during full-power operation of the radar transmitter.
- (U) ~~(S-NF)~~ *Results:* Spectral noise level on simulated clutter was at least 80 dB down, while clutter-related noise on actual clutter was only 60 to 70 dB down.
- (U) *Frequencies:* 17.4, 18.4, and 22.1 MHZ.
- (U) *Dates:* June 2, 3, and 9, 1972.

Test 10: Receiver Attenuation(25)

- (U) *Description:* Attenuate received ground clutter from beam 7 at the receiver input in 6-dB steps to 30 dB.
- (U) ~~(S-NF)~~ *Results:* Clutter and clutter-related noise at the signal processor output were linear with receiver attenuation, indicating that receiver overload was not a source of clutter-related noise.
- (U) *Frequency:* 17.4 MHZ.
- (U) *Date:* June 3, 1972.

(U) ~~(S-NF)~~ Next, a number of tests of the radar antenna on reception are described. Spectrally clean test signals were radiated toward the radar antenna from various points in the local area, and the received signals were examined for spectral noise of a level comparable to the observed clutter-related noise. One might note that extensive rework of the antenna was undertaken by the contractor (RCA) from Aug. 4 to Sept. 17, 1972. Antenna tests before the repairs were made showed a higher level of spectral noise than subsequent tests, which tended to exonerate the reworked antenna as the principal cause of clutter-related noise.

Test 11: Loop Antenna at the Focal Point(25)

- (U) *Description:* Radiate a simulated clutter signal from a loop antenna located at the geometrical focal point of the radar antenna. Receive on beam 1 with vertical polarization.
- (U) *Results:* Spectral noise was observed 60 to 70 dB down from the simulated clutter. A similar level of clutter-related noise was simultaneously observed on actual ground clutter, with the radar transmitter operating at full power during the test.
- (U) *Frequency:* 22.2 MHZ.
- (U) *Date:* June 9, 1972.

Test 12: Monopole Antenna on Sea Wall(25)

- (U) *Description:* Radiate a test signal from the vertically polarized monopole. Receive on beam 13 with alternating horizontal and vertical polarization.
- (U) *Results:* Spectral noise was down 80 dB when receiving vertical polarization, but down only 45 dB (at 20.6 MHZ) to 70 dB (at 39 MHZ) when receiving horizontal polarization, that is, when cross polarized.
- (U) *Frequencies:* 20.6, 24.2, and 39 MHZ.
- (U) *Dates:* July 6 and 7, 1972.

Test 13: Vertical Dipole on Sea Wall(21)

- (U) *Description:* Radiate a test signal from a vertically polarized dipole. Receive on beam 13 with vertical polarization.

- (U) *Results:* Spectral noise on test signal was down 91 to 95 dB from carrier.
- (U) *Frequency:* 20.135 MHz.
- (U) *Date:* Sept.21, 1972.

Test 14: Helicopter-borne Test Antenna (20,21)

- (U) *Description:* Suspend a 1-watt CW transmitter and a vertical dipole antenna 300 ft. below a helicopter hovering at 500 to 1000 ft. in altitude about 1/2 mile from the radar antenna. Receive the signal with the radar antenna in vertical polarization and measure spectral noise level,
- (U) *Results:* Spectral noise level was down 82 to 90 dB from the carrier of the CW test signal.
- (U) *Frequency:* 25.1 MHz..
- (U) *Dates:* Oct.26 and 27, 1972.

Test 15: SAC Test 1 - Monopole on Sea Wall (26)

- (U) *Description:* Radiate a test signal from a Fluke frequency synthesizer through a vertically polarized monopole antenna mounted on the sea wall. Receive this signal in turn on strings 4, 13, and 16 with vertical polarization.
- (U) *Results:* Spectral noise on received test signal was down 86 to 106 dB at 15 HZ from the carrier frequency. Noise level decreased with carrier frequency and had some correlation with wind velocity.
- (U) *Frequencies:* 8, 11, 16 and 23 MHz.
- (U) *Dates:* April 12 through 27, 1973.

Test 16: SAC Test 1 - Airborne One-Way Measurements (26)

- (U) *Description:* Radiate a CW test signal from an antenna trailed behind an aircraft orbiting 4 mi from the radar at 4,000-ft altitude. Receive on string 15 of the radar antenna.
- (U) *Results:* spectral noise was down 88 to 92 dB from the carrier on four passes during calm wind conditions.
- (U) *Frequency:* 23 MHz.
- (U) *Date:* March 21, 1973.

(U) The next group of tests involved simultaneous testing of the transmitting and receiving chains of the radar, utilizing either a specially constructed signal repeater in the local area or actual ground clutter from OTH ranges. Although the radar antenna both transmitted and received during these tests, in some cases a supplemental nine element Yagi-Uda test antenna (27) was also used so that a comparison with the radar antenna could be made.

Test 17: Repeater on the Sea Wall (28)

- (U) *Description:* A signal repeater with a 1/8 wavelength monopole receiving antenna, delay line, amplifier, and 1/4 wavelength monopole-transmitting antenna, was placed on the sea wall. The radar was operated normally, except that transmitter power was reduced 21 dB.
- (U) *Results:* Spectral noise of the repeated signal at the signal processor output was down 85 dB from the carrier.
- (U) *Frequency:* 27.5 MHz.
- (U) *Date:* Oct. 4, 1972.

Test 18: SAC Test 1 - Aircraft Repeater (26)

- (U) *Description:* The above repeater was placed in an aircraft, which orbited 4 miles from the radar at 4,000-ft altitude. Transmission and reception were alternated from string 15 of the radar antenna with horizontal polarization and the Yagi-Uda test antenna, which was also horizontally polarized.
- (U) *Results:* Spectral noise of the repeated signal was down 79 to 85 dB on string 15, and down 77 to 83 dB on the Yagi antenna.
- (U) *Frequency:* 23 MHz.
- (U) *Date:* March 27, 1973.

Test 19: Transmitter Power Reduction (25)

- (U) *Description:* Reduce transmitter power in 3-dB steps to 12 dB, during normal radar operation in beam 7 with horizontal polarization.
- (U) {(S-NF)} *Results:* Received ground clutter and clutter-related noise were both linear with transmitter power.
- (U) *Frequency:* 17.4 MHz.
- (U) *Date:* June 3, 1972.

Test 20: SAC Test 2 - Subclutter Visibility with an Auxiliary Antenna. (29)

- * (U) {(S)} *Description:* Alternately transmit and receive on string 16 of the radar antenna and the nine-element Yagi-Uda test antenna. Compare the ratios of ground clutter to clutter-related noise obtained with each.
- (U) {(S)} *Results:* With string 16, the clutter-related noise was 68 to 77 dB below the ground clutter on three different days. With the Yagi-Uda antenna, the clutter-related noise was 71 to 77 dB below the ground clutter. Day-to-day variation was greater than that between antennas.
- (U) *Frequency:* 23 MHz.
- (U) *Date:* March 8, 14, and 16, 1973.

EQUIPMENT COMPONENTS AS POSSIBLE SOURCES OF CLUTTER-RELATED NOISE

(U) ~~(S)~~ All components of the radar, including its local environment, were considered as possible sources of clutter-related noise. For each component, one or more physical mechanisms capable of generating clutter-related noise were hypothesized. These mechanisms (see Table 5) were then considered in structuring the equipment tests for clutter-related noise. Table 6 summarizes the results of the 20 equipment tests as described earlier with respect to sources of clutter-related noise in each radar component. A minus sign (−) means that a given radar component was found not to be a significant source of clutter-related noise; a plus sign (+) means that a component was found to be significant. Many squares in the table are left blank, indicating no conclusive relationship between a given equipment test and a given radar component.

(U) ~~(S)~~ Spectral noise on the radar transmitter output could cause clutter-related noise to appear on ground clutter. The ratio of clutter to clutter-related noise expected would be approximately equal to the ratio of carrier to spectral noise on the transmitter output, if such spectral noise were the principal cause of clutter-related noise. The transmitter noise level measurement (Test 1) showed a very low level of spectral noise—much too low to account for the observed clutter-related noise. A test using a fan dipole on the sea wall (Test 3) also showed transmitted spectral noise to be much lower than the generally observed clutter-related noise. The two overall system tests using a repeater (Tests 17 and 18) also tended to clear the transmitter as a cause of clutter-related noise. Finally, the observed linearity of clutter-related noise with transmitter power (Test 19) was an indication that nonlinear effects in the transmitter were not a significant source of clutter-related noise.

(U) ~~(S)~~ Receiver testing was more extensive than transmitter testing, in part because numerous tests of the radar antenna also implicitly tested the radar receiver. Tests of receiver linear dynamic range, intermodulation distortion, and cross-modulation distortion (Tests 4, 5, and 6) showed that the spectral noise imposed upon received ground clutter by these receiver phenomena should be much lower than the levels of clutter-related noise actually observed, thus showing that the receiver was not the major cause of clutter-related noise. The electromagnetic interference measurements (Test 8) showed that out-of-band electromagnetic interference occasionally exceeded receiver ratings, which could allow cross modulation in the receiver to cause significant clutter-related noise. However, such large out-of-band electromagnetic interference was rare, whereas clutter-related noise was observed all the time when ground clutter was strong. Testing of the receiver with simulated clutter (Test 9) showed spectral noise on the simulated clutter to be smaller than observed clutter-related noise on actual clutter received at the same time. Actual clutter and clutter-related noise were also shown to be linear with received signal attenuation (Test 10), thus indicating that receiver overload was not a cause of clutter-related noise.

TABLE 5. *Physical mechanisms for clutter-related noise. (Table unclassified.)*

Radar Component	Physical Mechanisms
Transmitter	Spectral noise on carrier
Receiver	Intermodulation distortion; cross-modulation distortion
Signal Processor and Displays	A/D converter transient response Insufficient dynamic range Spectral aliasing
Antenna, ground screen, and RF Hardware	Wind vibration of radiating elements Wind vibration making and breaking contacts Arcing and corona Cross modulation in nonlinear joints
Local Environment	Cross modulation in ancillary electrical equipment Sea scattering from first Fresnel zone

(U) ~~(S)~~ Antenna reception Tests 13 through 16 included the receiver in the test chain. Since low levels of spectral noise were observed, these tests also exonerated the receiver as the principal cause of clutter-related noise. For example, the test employing a vertical dipole on the sea wall as a signal source (Test 13) showed spectral noise down 91 to 95 dB from the carrier, which is far lower than the clutter-related noise-to-clutter ratios commonly observed. Transmit and receive system tests employing a signal repeater (Tests 17 and 18) also tended to exonerate the receiver, although the spectral noise in these cases was not quite so low, because of the limitations of the repeater.

Radar Component Test	Transmitter	Receiver	Signal Processor and Displays	Antenna, Ground Screen, and RF Hardware				Local Environment Including Sea
				Before Rework		After Rework		
				On Transmission	On Reception	On Transmission	On Reception	
1 Transmitter Noise Level	-							
2 Fan Dipole on Sea Wall #1						+		
3 Fan Dipole on Sea Wall #2	-					-		
4 Receiver Linear Dynamic Range		-						
5 Receiver Intermodulation		-						
6 Receiver and Duplexer Cross Modulation		-		-	-			
7 Radio-Frequency Hardware Measurements							-	
8 EMI measurements		-						
9 Simulated Clutter into Receiver		-	-					
10 Receiver Attenuation		-	-					
11 Loop Antenna at Focal Point					+			
12 Monopole Antenna an Sea Wall					+			
13 Vertical Dipole on Sea Wall		-	-				-	
14 Helicopter-Borne Test Antenna		-	-				-	-
15 SAC Test 1- Monopole on Sea Wall		-	-				-	
16 SAC Test 1 - Airborne One-Way Measurements		-	-				-	-
17 Repeater on Sea Wall	-	-	-			-	-	-
18 SAC Test 1 - Aircraft repeater	-	-	-			-	-	-
19 Transmitter Power reduction	-			-				
20 SAC Test 2 - Clutter and CRN with Auxiliary Antenna						-	-	-

(U) ~~(S)~~ The receiving chain and signal repeater tests also indicated that the radar signal processor and displays were not the cause of clutter-related noise. That is, spectrally clean test signals injected ahead of the signal processor were observed on the displays to be not corrupted with spectral noise to anything near the level of clutter-related noise observed on actual ground clutter. There was a further indication that all the radar signal processor circuits after the analog-to-digital converter had adequate linear dynamic range to properly spectrum-analyze ground clutter. An off-line digital signal processor was developed by MITRE[19] to supplement the on-line hybrid digital/analog radar signal processor. Careful comparison of clutter-related noise at the output of the off-line digital processor with clutter-related noise observed on the radar displays showed very close agreement in amplitude, spectrum, and time variation. While it is possible that both processors might have had an undetected flaw, it is extremely unlikely that both would have had exactly the same flaw.

(U) ~~(S)~~ A lingering doubt does exist about one component of the signal processor—the analog-to-digital converter. A colleague[20] has put forth the hypothesis that analog-to-digital converter transient response errors in following time-varying clutter might account for the spectrally spread clutter-related noise. Since all test signals, both cw and pulsed, had constant amplitude from one radar pulse repetition interval to the next, the transient response of the analog-to-digital converter may not have been adequately tested, according to this hypothesis. At this late date, there appears no way to resolve this question.

(U) ~~(S)~~ Four tests of the radar antenna, ground screen, and RF hardware were conducted in the spring and summer of 1972, before RCA reworked these components. The transmitter power reduction test 19 tended to rule out nonlinear effects in the transmitting antenna, such as arcing and corona, as the principal cause of clutter-related noise, but it was too limited in scope to be wholly conclusive. Cross-modulation distortion in the duplexers was measured in conjunction with similar receiver measurements (Test 6) and found to be negligible. Two early tests of the antenna on reception gave positive results, however. Spectrally clean test signals that were radiated from a loop antenna at the geometric focal point of the radar antenna (Test 11) showed spectral noise at the signal processor output comparable in amplitude to the clutter-related noise simultaneously observed on ground clutter. When a vertical monopole on the sea wall was used to radiate a spectrally clean test signal (Test 12) to the radar antenna, spectral noise was also observed at the signal processor output. With the radar antenna vertically polarized, spectral noise on the test signal was lower than the clutter-related noise usually observed on ground clutter. However, with the radar antenna horizontally polarized (cross polarized to the test signal), spectral noise on the test signal at some frequencies was higher than the clutter-related noise usually observed on ground clutter. The results of these two tests were taken as an indication that at least some of the clutter-related noise was originating in the radar antenna on reception—possibly in the ground screen, because it could produce cross-polarized spectral noise.

(U) As a result of these early antenna tests, a team of engineers from RCA Moorestown, the AN/FPS-95 contractor, came to the site in the fall of 1972. They inspected the antenna, ground screen, and RF hardware, had extensive repairs and rework done, and then participated in further tests of the reworked antenna. Rework of the antenna was conducted between Aug. 4 and Sept. 17, 1972. Expansion sections in the RF hardware and the ground screen clips were both found to generate spectral noise during two-tone intermodulation tests; corroded joints were also found by visual inspection. The expansion sections were replaced, steel towers in the antenna field were rewelded to reduce nonlinear RF effects at joints, grounding connections were improved, and the ground screen clips were welded. Coaxial lines to the baluns were modified and grounded, as were certain conduits and fan plates. All loose metal debris in the antenna field was removed.

(U) After the rework, extensive testing of the antenna on both transmission and reception was performed. Transmitting tests were directed toward both linear sources of spectral noise, such as wind vibration, and nonlinear sources, such as arcing and corona. Receiving tests took into account wind vibration also, as well as nonlinear effects, such as rectifying action at joints in the antenna and ground screen.

(U) {(S)} Transmission from the radar antenna to a fan dipole on a sea wall (Tests 2 and 3) showed low spectral noise when the radar antenna and test antenna had the same polarization, but higher spectral noise when the two antennas were cross polarized. This indicated that some spectral noise generation mechanisms still existed in the antenna on transmission, especially at the lower operating frequencies, but that these were probably not the principal cause of clutter-related noise. In this regard, it should be noted that the spectral noise uncovered in cross-polarization testing was concentrated in the region of 10 to 30 HZ from the carrier, whereas clutter-related noise associated with ground clutter had a spectrum that fell off slowly, but monotonically, with Doppler shift. While cross-polarization testing was a good way to uncover spectral noise generation mechanisms in the antenna, it differed too much from normal radar operation to be readily interpreted in terms of the clutter-related noise that could be expected on actual ground clutter. The two repeater tests of the whole radar system (tests 17 and 18) showed no noise generation in the antenna, within the limits of the instrumentation. Finally, a comparison of clutter to clutter-related noise ratios between one string of the radar antenna and an auxiliary test antenna having a roughly similar radiation pattern (Test 20) showed no significant differences. This was a further indication that the radar antenna was not the principal cause of clutter-related noise.

(U) {(S)} Several reception tests were also performed on the reworked antenna. The RF hardware measurements (Test 7) showed no significant source of clutter-related noise, unless the level of electro-magnetic interference at the antenna terminals approached 0 dBM, which rarely occurred. Spectrally clean test signals were radiated toward the receiving antenna (Tests 13 through 16) from the sea wall, from a helicopter, and from an aircraft. The sea wall provided a stable mounting point for a test antenna, allowing very low levels of spectral noise (more than 90 dB down from the carrier) to be observed at the signal processor output. However, the sea wall was not in the far field of the antenna and was lower in elevation than either of the radar elevation beams. The helicopter and aircraft tests were intended to get further from the antenna and in the main lobe of one of the radar elevation beams. These tests also showed the radar antennas on reception to be relatively free of spectral noise generation, but not to the degree of the sea wall tests, because the airborne platforms were not sufficiently stable. It might be noted that some of these tests were done on windy days, so the hypothesis that wind vibration of radar antenna elements caused clutter-related noise was thoroughly tested. Wind vibration was shown to produce some spectral noise, but was a minor contributor to the observed levels of clutter related noise.

(U) {(S)} The local environment of the radar system was included in some of the equipment tests for clutter-related noise. Receiving chain tests with the helicopter-borne test antenna (Test 14) and the airborne one-way measurements (Test 16) included some of the sea within the first Fresnel zone of the antenna ground plane. Most of the first Fresnel zone was within the aircraft test range of 4 miles; only part was within the helicopter test range of 1/2 mile. Both of these tests showed received spectral noise almost 90 dB down from the carrier at the Doppler frequencies of interest. Apparently, significant modulation of the signal by sea waves was confined to smaller Doppler shifts. The low level of spectral noise observed during these tests also negated the hypothesis that clutter-related noise might be caused by cross-modulation effects in ancillary equipment near the radar site, such as transmission lines, power stations, and so on.

(U) {(S)} The aircraft repeater measurements (Test 18) were conducted with the repeater at a range of 4 miles from the radar. These measurements uncovered no spectral noise that could be attributed to the local environment. Because of instrumentation limitations, this test was not quite as conclusive as the one-way receiving chain tests. Both the aircraft repeater test and the auxiliary antenna measurements (Test 20) made use of a Yagi-Uda antenna located about 1/2 mile south of the radar antenna. During these tests, no significant differences in spectral noise on test signals or in clutter related noise on ground clutter were found between the two antennas. This was a further indication that local environmental effects, which were some what spatially decorrelated between the two antennas, were not the principal cause of clutter-

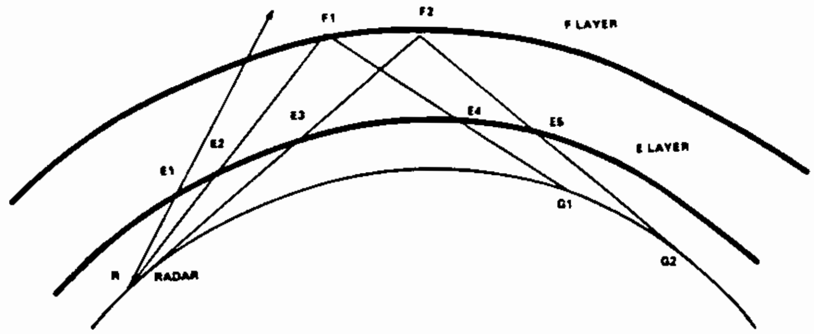

Figure 15. Ray path geometry. (Figure unclassified.)

related noise. One further piece of evidence—the absence of nonlinear effects during the transmitter power reduction Test 19—tended to negate the hypothesis of cross modulation in ancillary equipment.

CONCLUSIONS OF EQUIPMENT TESTING

(U) ~~(S)~~ Numerous tests of the AN/FPS–95 transmitter showed it to have exceptional spectral purity and to be a negligible contributor to the overall level of clutter-related noise. The radar receiver, always a prime suspect as the cause of clutter-related noise, was very thoroughly tested for spectral noise generation. It, too, was exonerated, except when very large out-of-band interferers were present at the receiver input. Since such interferers were rarely present, whereas clutter-related noise was always present when OTH propagation was good, it was concluded that the radar receiver was not the principal cause of clutter-related noise. The radar signal processor was shown through numerous tests to not be a significant source of clutter-related noise. A minority opinion(30) would have it that these tests did not adequately measure the analog-to-digital converter transient response to time-varying clutter.

(U) ~~(S)~~ Some spectral noise generation mechanisms were found in the AN/FPS–95 antenna, ground screen, and RF hardware. After extensive rework of these components by RCA, such noise generation mechanisms were considerably reduced, but still present. Extensive system testing on both transmission and reception showed that the antenna, ground screen, and RF hardware were not the principal cause of clutter-related noise. These components had particularly good spectral purity above 20 MHZ, whereas clutter-related noise on actual ground clutter was just as prevalent as it was at lower radio frequencies. Some tests of the radiating system also included its local environment, particularly the sea. The local environment seemed no significant source of such noise.

(U) ~~(S)~~ Having rather thoroughly exonerated the radar equipment as the limiting source of clutter-related noise, attention turned to factors external to the radar. Both the ionospheric propagation medium and radar reflectors in the target space were considered as sources of clutter-related noise, as discussed in the next section.

THE SEARCH FOR SOURCES OF EXCESS NOISE IN THE EXTERNAL ENVIRONMENT

(U) After an introductory discussion of propagation geometry, this section gives brief descriptions of all the relevant experiments and tests, followed by discussions of postulated causes of noise due to reflection effects and propagation phenomena.

PROPAGATION GEOMETRY

(U) ~~(S)~~ Figure 15 shows an idealized diagram of the propagation ray paths typical of radar operation using the ionosphere F-layer as the reflecting layer (the normal mode of operation). The rays emanating from the radar located at R are shown as being restricted to a range of elevation angles bounded by the lower ray path R–E3 and the upper ray path R–E1. In fact, of course, the actual elevation gain pattern did not have such sharp boundaries. It featured a direction of maximum gain that could be switched between an upper elevation angle of approximately 15 deg and a lower position of typically 5 to 7.5 deg by selecting, respectively, horizontal and vertical polarizations. The measured antenna patterns indicated considerable variations in elevation beam shape as a function of beam number and radar frequency.

UNCLASSIFIED

S[redacted]N

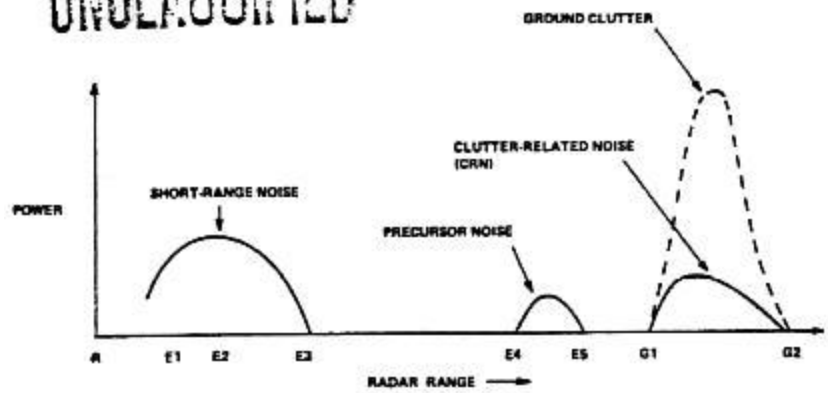

Figure 16. Radar-range relationships.
(~~Figure classified Secret.~~ (U))

(U) The radiation pattern gain did approach zero at a zero elevation angle, due to horizon shielding, but there was considerable antenna gain at angles higher than the nominal upper limit of the beam represented by ray path R-E1. The effect of the high-angle radiation was not usually important, however, since these rays would normally pass through the F-layer end thus would not contribute to the normal OTH radar process. In Fig. 15, the highest ray that is reflected from, rather than penetrating, the F-layer is shown by the ray path R-F1-G1. This ray is shown as passing through the E-layer at points E2 and E4. Similarly, the lowest ray follows the path R-F2-G2 and intersects the E-layer at E3 and E5. The ionospheric layers do not behave exactly as simple mirrors, as indicated in Fig. 15. The effective reflection heights, such as those of points F1 and F2, are a function of the radar frequency, the incidence angles of the radiation, and the ion density profile. Usually, at a fixed frequency the rays having the larger elevation angles at the radar will penetrate higher. Thus, point F1 would be slightly higher than F2. This phenomenon gives rise to a focusing effect, with the result that the effective gain of the antenna, when viewed looking back up the ray path from the region following the ionospheric reflection, is modified from that of the prereflection region. Usually, the effect is to increase the gain along rays in the region close to the uppermost ray (F1-G1). Figure 16 shows, along the abscissa, the relative time delays from the radar for reflections assumed to occur at the labeled points corresponding with the notation in Fig. 15.

(U) The radar-range dependence of the observed amplitude of OTH ground clutter, as sketched in Fig. 16, may be accounted for as follows. On the radar side of point G1, no ground reflections are possible, because the ionosphere does not reflect the rays leaving the radar at elevation angles higher than that of R-F1. Moving from point G1 away from the radar, the ground reflections, as received back at the radar, build up in a particularly abrupt manner, since this is the region of enhanced gain due to the ionospheric focusing action. Beyond this point, the combined effects of increasing range, reducing antenna gain, and diminishing earth-grazing angle produce a rapid reduction in the received backscatter amplitude. For the depicted one-hop propagation mode, the ground backscattcr should effectively disappear at ranges greater than that appropriate to the point G2.

DESCRIPTION OF EXPERIMENTS AND OBSERVATIONS

Synoptic Measurements

(U) {(S)} During the approximately 18-month life of the AN/FPS-95, many observations were made and recorded in the form of notes, photographs, computer printouts, and magnetic tapes. Much of this information was relevant to the investigation of clutter-related noise. Unfortunately, these data were taken using a variety of radar operating parameters and analyzed by a number of different methods. The consequence was that the usefulness of the data for investigating the relationship between clutter-related noise and any single radar or operational parameter was impaired.

(U) {(S)} To supplement the above data base, during the clutter-related noise investigation of the Scientific Assessment Committee, a concentrated synoptic data-gathering activity was conducted during February 1973 for a period of 19 days.(31) A daily schedule of 12 data-gathering runs was made on each of beams 1, 7, and 12. During and beyond the duration of this test, local weather, solar flux, and the geomagnetic index were recorded to permit the investigation of possible correlation with clutter-related noise. The results of synoptic test data analysis clearly confirmed the persistent existence of the short-range, precursor, and clutter-related noises. They did not, however, reveal any clear correlation between the clutter-related noise and local weather, solar, or geomagnetic parameters.

(U) ~~(S)~~ An interesting effect noted in data recorded between September 1972 and May 1973 is that the ratio of ground clutter to clutter-related noise appeared to vary distinctly as a function of beam azimuth. The relative amount of noise was lowest in beam 1, rose gradually through beam 9, then dropped again until the most southerly beam 13 was reached.[32] The maximum variation (beam 1 to beam 9) was approximately 10 dB.

Land/Sea Test[33]

(U) ~~(S)~~ The object of this test was to investigate the hypothesis that the clutter-related noise was generated, through the modulation and backscattering of radar energy, by objects situated on or near the earth's surface, at ranges normally illuminated by the one-hop OTH radar propagation modes. Because of the importance of this experiment and its results, it is described in greater detail in the appendix at the end of this paper.

(U) ~~(S)~~ The test was arranged to measure the clutter-related noise powers from range–azimuth resolution cells within an area of AN/FPS–95 coverage encompassing both land and sea areas. The greatest variations in clutter-related noise levels were found to occur between adjacent land and sea areas. These results were not inconsistent with the assumption that no clutter-related noise was generated within the resolution cells located over the sea.

Short-Range Noise Test[34]

(U) The primary purpose of this test was to identify the sources of the component of range-related noise observed to occur at short radar ranges (less than approximately 600 nmi). The particular postulated mechanisms investigated were transmit/receive switch transients, transmitter-induced corona, antenna vibration, and meteor effects.

(U) Examination of off-line processed data showed that the switching transient effects were confined to extremely short radar ranges and that they could be ignored at the ranges of the observed short-range noise. Earlier in the AN/FPS–95 testing program, the presence of more serious switching transients had been observed using the on-line signal processor. These were subsequently reduced by an equipment modification. In this connection, it should be noted that the vast majority of data used in the investigations of range-related noise were analyzed by off-line techniques.

(U) Although antenna arcing had previously been observed at lower radar operating frequencies, measurements at 23 MHz, the frequency used for most short-range noise tests, failed to reveal any evidence of the phenomenon.

(U) A measurement made at a frequency of 23 MHz in beam 13 using vertical polarization contained a surface wave clutter signal at a range of 40 nmi. The amplitude of this signal was sufficiently higher than the noise background of the spectrally analyzed data to permit the conclusion that any spectral spreading of the signal (by antenna vibration) would be down by at least 66 dB. This conclusion does not, of course, necessarily exonerate the antenna at other frequencies, beam positions, and polarizations.

(U) ~~(S)~~ The main effort in this test was devoted to an examination of the meteor theory of short-range noise generation. The noise was recorded in beam 1 and beam 13 for each of the two available antenna polarizations (vertical and horizontal). Changing the polarization had the effect of raising the beam from a lower position to a higher position. The radar ranges of the recorded short-range noise were seen to shift in toward the radar when the beam was raised, in accordance with the hypothesis of backscattering occurring within the E-layer. The recorded data were used to calculate the antenna vertical beamshape for subsequent comparison with independent measured patterns. A good correspondence was thus obtained. The above measurements were performed both above and below the maximum usable frequency, at a frequency of 23 MHz, by choosing the appropriate diurnal time. Some of the measurements, when operation was below the maximum usable frequency, were made at a low pulse repetition rate

(10 HZ). These latter data showed, incidentally, the typical appearance of precursor noise and clutter-related noise.

Auroral Measurements

(U) As part of the planned experimental activity, a large quantity of data on the radio auroral effects was gathered during the life of the AN/FPS-95. This was taken from observations in the northerly beams (numbers 1 through 6). (12) In addition, the data recorded during the special synoptic investigation of clutter-related noise from beams 1, 7, and 12 were likewise examined for their auroral contributions. (12)

(U) {(S)} Although the results showed that, particularly in the most northerly beams, auroral radar echoes could adversely affect the performance of the AN/FPS-95, there was no indication that these effects were related in any way to the clutter related noise, which by observation and definition, and in contrast to the auroral returns, always occurred at the same radar ranges as the earth surface backscatter.

One-Way OTH Path Test (35,35)

(U) {(S-NF)} Objectives of the One-Path Test were (*1*) to determine whether the spectrum of a known "clean" signal would be modified by effects associated with propagation via an ionospheric path and (*2*) to compare the signal received by various components of the AN/FPS-95 antenna (the antenna employed a ground screen thought to be a possible cause of clutter-related noise) with the signal received by specially constructed Yagi antenna. Aimed toward the Eastern Mediterranean, the antenna pattern resembled that of a single string of the AN/FPS-95 antenna. The Yagi had no ground screen.

(U) {(S-NF)} In the tests, which were performed for the 6-day period from March 6 to 11, 1973, signals were transmitted by the AN/FPS-95 in England and received in the Eastern Mediterranean, and signals were transmitted by an HF site in the Eastern Mediterranean and received in England. During the period of the tests, the HF site transmitted for a 2-hr period from 10:00 a.m. to 12:00 noon. The interval was broken up into eight 15-min periods, during each of which the transmitter at the HF site was turned off during the fifteenth minute to permit the receive antenna configuration at the AN/FPS-95 to be changed. The Yagi was used during the first and last 15-min periods; in between, combinations of the two strings of the AN/FPS-95 antenna that pointed toward the HF site in the Eastern Mediterranean were used so that comparisons could be made. During the following 2-hr period, from 12:00 noon to 2:00 p.m., the AN/FPS-95 transmitted and the signal was received in the Eastern Mediterranean by means of a gated receiver installed in a van located near the HF site. The dynamic range of the gated receiver and processor was 80 dB or more. All one way tests were performed at 23.145 MHZ.

(U) {(S-NF)} The shape of the spectrum of the signal received at the AN/FPS-95 was essentially the same as that transmitted from the HF site at the same time. The spectrum was clean down to a level above 70 dB below the peak, at which point skirts formed; the average level of the skirts then fell off with frequency on either side of the carrier. Lines seen at a number of discrete frequencies in both local and over-the-horizon spectra were related to the power frequency and to blower frequencies. No evidence of any contamination by the ionosphere is present in the spectrum received at the AN/FPS-95, and no differences of consequence were seen between the spectra received by the several receive antenna configurations used at the AN/FPS-95, indicating that the ground screen of the system antenna was not contributing measurable noise. The spectrum of the AN/FPS-95 signal received at the HF site likewise was found free of noise down to the limit of dynamic range of the gated receiver, which was about 83 dB.

Sporadic-E Layer/F-layer Test (37)

(U) {(S)} The objective of the Sporadic-E Layer/F-layer Test was to explore whether one layer or another of the ionosphere was the unique cause of the observed clutter-related noise. The test was made in connection with the Scientific Assessment Committee program in the early part of 1973 relative to the Synoptic Data Task (Task 7).

(U) {(S)} The idea of the test was to compare the spectra of signal sequences that propagated via two-way sporadic-E refraction paths with the spectra of signal sequences that propagated simultaneously via two-way F-layer refraction paths. If the spectra of the signal sequence that propagated via

F-layer contained clutter-related noise and that via sporadic-E did not, then the F-layer as a possible unique cause of clutter-related noise could be inferred; if the signals that propagated via sporadic-E only had clutter-related noise and the F-layer-only signals did not, then the F-layer would be absolved and sporadic-E implicated, and so on. Because sporadic-E layers were not in evidence during the time interval within which the Scientific Assessment Committee's investigation was conducted (February and March 1973), use was made of data recorded in June 1972 in connection with Design Verification System Testing (DVST) Experiment 202, when sporadic-E was a frequent occurrence.

(U) ~~(S)~~ Analysis of the data showed clutter-related noise to be present in the spectra of signal sequences that propagated over two-way sporadic-E propagation paths and in the spectra of signals that propagated simultaneously over two-way F-layer paths. The characters of the noise and the clutter-to-noise ratios were roughly the same in the two cases.

Transmitter Power Reduction Test [25]

(U) ~~(S-NF)~~ Objective of the Transmitter Power Reduction Test which is relevant here was to determine whether the high power radiated by the transmitter was heating, and thus modifying, the ionosphere so as to cause the observed clutter-related noise.

(U) ~~(S-NF)~~ The test was done by members of the on-site staff on June 3, 1972 with the radar in its normal operating configuration, transmitting in beam 7 on horizontal polarization at a frequency of 17.4 MHz. All six transmitters were used. The transmitter power was reduced in steps of 3, 6, 12, and 18 dB, each step being maintained for one minute, and all measurements were taken within about 5 min. In the data processing, range bins 80 nmi in range extent were formed, and the returns in each was coherently integrated for 6.4 sec. Further processing then yielded average noise power in all Doppler bins from PRF/8 to PRF/2 and the average clutter power in the first eight Doppler bins around the carrier frequency. These averages were computed for each range bin during each integration interval.

(U) ~~(S-NF)~~ The result relevant here is the behavior of average clutter power and average noise power in a range bin set near the peak of the ground backscatter. Here the clutter power and noise power decreased together as transmitter power was decreased, but clutter and noise were only 10 to 12 dB down for the transmitter power reduction of 18 dB. (The experimenter conjectured that poor calibration of the power reduction switch could have caused the discrepancy.) There was no *sharp* reduction in noise power at any point during transmitter power reduction. Both clutter power and noise power decreased smoothly and proportionately with transmitter power reduction.

REFLECTION EFFECTS

(U) ~~(S-NF)~~ Postulated causes of range-related noise which attribute the phenomenon to equipment, local environment, or propagation effects generally include the assumption of the earth-surface reflection as an element of the relevant two-way radar propagation paths. This reflection is regarded as that of a fixed reflector, however, which does not therefore alter the spectral composition of the reflected energy from that of the incident energy. The spectral broadening that accounts for the clutter-related noise is assumed to occur elsewhere. In contrast, this section discusses postulated causes of range-related noise in which the spectral broadening of radiation, which is reflected back to the radar receiver from distant locations, occurs at the actual point of reflection. This reflection point may be in the normal ground-clutter reflection area or at some totally different location.

(U) ~~(S-NF)~~ As described previously and as seen in Fig. 16, the range-related noise was observed mainly in three well-defined regions of radar range, that is, a "short-range" region extending out to approximately 600 nmi, a "precursor" region in front of the ground-clutter return, and a region coincident with the ground-clutter return. This latter noise is named "clutter-related noise," and it is the one of highest importance in its effect on the observation of most aircraft, since it is at the ranges of the ground clutter that the lower atmosphere is illuminated and, consequently, where the aircraft echoes are to be found. The other regions are also of some interest, however, since their noise may obscure the OTH observations of high-altitude targets such as ballistic missiles, as well as those of target echoes generated via multi-hop ambiguous-range propagation modes. Yet

Table 7. *Reflection effects matrix. (Table unclassified.)*

Observation	Synoptic Observations	Land/Sea Comparison	Sporadic E/F layer Comparison	Short-Range Noise Test	Auroral Measurements
Postulated Cause					
Meteors	**X**	**X**		**X**	
Auroral Effects					**X**
Aircraft Returns	**X**				
Earth-Surface Effects		**X**	**X**		
MultiHop Reflections	**X**			**X**	

another reason for investigating the origin of the close-in and precursor noise was the possibility that there may have been a single common cause for all of the observed excess noise.

Postulated Reflective Causes of Range-Related Noise

(U) Possible explanations for the generation of range-related noise attributed to reflection mechanisms, together with the relevant observations that tend to support or disprove the theories, are listed in Table 7 and are discussed in the following paragraphs.

Meteors

(U) {(S)} It has long been known that meteors entering the lower ionosphere at heights of around 100 km produce ionization effects that reflect radio waves in the high frequency radio band. (38) Since these meteor-induced effects are transitory in nature and would therefore spread the spectrum of the incident radiation, they were obvious suspects as the cause of at least some of the range-related noise. Figures 15 and 16 show how the presence of the meteor reflections in the E-layer can give rise to the range-related noise identified as "short range" and "precursor." The meteor effects would be distributed evenly through the E-layer, thus resulting in a precursor range- related noise power-versus-range profile very similar in shape to that of the ground clutter, but reduced somewhat in range. Both theory and experiment have previously shown that the close-in and precursor range related noise should and does exist. (39,40) Furthermore, the calculated and observed spectra of these features are shifted toward the recede direction, a fact that is in agreement with observations made with the AN/FPS-95. Figure 15, for clarity, exaggerates the vertical scale. In fact, the far tail of the precursor range-related noise would overlap the area G1-G2 occupied by the ground clutter and thus come under the definition of clutter-related noise. However, it would not give rise to a peak of noise within this region, as observed with the AN/FPS-95 and depicted in Fig. 16, and would not exhibit the symmetrical spectrum of the observed clutter-related noise.

(U) {(S)} There were, and probably still are investigators who believe that the precursor noise and the clutter-related noise are one and the same phenomenon, This view is not shared by the authors of this paper. Strong credence was lent to the meteor explanation for the short-range noise by the results of the short-range noise experiment. (34) Evidence for the meteor explanation of the precursor range-related noise was less well established. However, one of the radar displays features an A-scope representation of the envelope of raw radar return signals, on which could often be observed the characteristic decaying transient signals typical of radar echoes from the ionized columns caused by meteorites. These transients occurred at the same ranges as the precursor noise, and the two phenomena were therefore assumed to be connected. The results of the land/sea experiment are not compatible with a meteor explanation of clutter-related noise, since it is highly unlikely that the meteor effects would exhibit abrupt differences in their reflection capabilities as a function of their geographical positions within the AN/FPS-95 coverage.

(U) ~~(S)~~ To summarize, it appears that the clutter-related noise is a different phenomenon from the close-in and precursor range-related noise, both of which appear to be caused by reflections of radar energy from meteor-induced ionization within the E layer.

Auroral Effects

(U) The term "auroral" is a very loose description of the postulated causes of clutter-related noise considered under this heading. Such causes include all those which may be attributed to radar reflections from ionospheric irregularities, whether magnetic-field-aligned or otherwise. It happens that most of such well-known effects occur in the high latitudes and are somewhat loosely correlated in position with visible aurora.

(U) ~~(S)~~ The radio aurora effects are known to produce radar reflections over a wide radio-frequency range, including the HF band. Furthermore, these reflections exhibit Doppler frequency shifts and spreading on the order of the observed clutter-related noise spectral widths. Over-the-horizon measurements in the Arctic have shown this "diffuse spectrum clutter" as a severe limitation to the detection of aircraft.(11) Also, the ranges from the AN/FPS-95 to the zone of maximum auroral activity were such as to place the radar ranges of the auroral reflections within the AN/FPS-95 coverage.

(U) ~~(S)~~ Much information was gathered throughout the operational life of the AN/FPS-95 on the radar returns from radio aurora.(12) In addition, more of these data were specifically gathered as part of the synoptic data collection during the investigation of clutter-related noise. These data clearly distinguished auroral effects from those of clutter-related noise in a number of particulars. First, the auroral returns, while occasionally coinciding in range with those of ground clutter, were generally to be found at ranges and with statistical frequencies that varied considerably, depending upon the time of observation, season, magnetic activity, operating frequency, and azimuth. Second, the spectra of the auroral backscatter were generally highly asymmetrical. And third, the amplitudes of the returns were found to depend strongly upon the radar frequency, being 10 to 30 dB higher at 8 MHz than at 10 MHz.

(U) ~~(S)~~ These observed characteristics of radio aurora reflections contrast strongly with characteristics of clutter-related noise, which include gradual variations in level as a function of beam azimuth and radar frequency, symmetrical spectra, and a close correlation in range with that of the ground clutter.

Aircraft Returns

(U) ~~(S)~~ Among the less plausible suggested causes of clutter-related noise was the possibility that the reflections from a large number of aircraft, entering the radar receiver through the antenna sidelobes, could be the source. It would be ironic indeed if the AN/FPS-95 failed to see aircraft because it was seeing too many aircraft! Quantitative calculations to examine this postulated phenomenon have not been performed, largely because of a lack of data concerning the numbers, velocities, and dispositions of aircraft about the radar. It does, however, seem extremely unlikely that within a given range cell, even within a large azimuth sector, there would have been sufficient aircraft to occupy all the Doppler cells (typically several hundred) and, thus, have given the appearance of broadband noise. Even if this had been the case, then the relatively small number of aircraft within the antenna mainlobe should have been separately resolvable in Doppler frequency and would, on account of the large two-way gain differential relative to the sidelobes, have been easily discerned above the clutter-related noise background. One would also have expected to see marked diurnal changes in the noise due to the reduction in air activity at night.

Earth-Surface Effects

(U) ~~(S)~~ While there are virtually no objects on the earth or sea surface which have translatory velocities comparable with those of aircraft and which might therefore produce Doppler-shifted radar reflections to interfere with OTH aircraft detection, there are nevertheless many objects, particularly man-made, that move, vibrate, or rotate in such a manner as to modulate an incident radio wave, either in phase or amplitude, so as to generate sidebands in the reflected power. These sidebands could, if removed sufficiently in frequency from that of the incident power, resemble clutter-related noise. Within a single AN/FPS-95 range-azimuth resolution cell (an area of approximately 10,000 nmi^2 for a 1-millisecond pulse at a range of 1,000 nmi) practically anywhere within eastern Europe, one would expect to find a large number of potential modulating reflectors, such as vibrating telephone wires, fences and power lines, rotating wheels, and moving vehicles which, either alone or through interaction with surrounding terrain or structures, would present time-modulated reflective properties. Qualitatively at least, it is plausible that such an ensemble of modulating entities could spread the spectrum of the incident radar energy to produce the clutter-related noise phenomenon. The assumption that these effects ere spread evenly throughout the AN/FPS-95 coverage would suffice to explain the observed correlation between the amplitude-versus-range behavior of the clutter-related noise and that of the ground clutter.

(U) {(S)} Another modulation effect could be generated by stationary reflecting objects, composed of sections between which the electrical impedance is varying. For example, the metal frameworks of buildings may be composed of sections that are poorly connected electrically. A mechanical vibration could cause such a connection to vary in impedance and thus produce a reflection with sidebands at the vibration frequency and its harmonics. Indeed, such an effect was used to calibrate the AN/FPS-95. The devices in question were located in Norway and Turkey and consisted of log-periodic antennas, pointing toward the radar, whose terminals were connected to modulated impedances. The reflected power from these switched reflectors, with its characteristic modulation frequency, could be detected and identified at the AN/FPS-95. It is possible to imagine many man-made artifacts that might conceivably contain such modulated impedances, including wire fences, vehicles, and even railroad tracks whose sections are connected by impedances that could vary rapidly during the passage of a train across the joints.

(U) {(S)} A third modulating agency, somewhat similar to that just described, involves the existence of nonlinear electrical impedances within the reflecting bodies. Such impedances, when exposed to local time-varying electrical fields, would also have the effect of modulating the reflections of incident radar energy, and thus have the potential for generating clutter-related noise.

(U) {(S)} Finally, it should be noted that the effects described here need not necessarily be limited to man-made reflecting bodies. Intuitively, however, the observed motions of natural objects such as vegetation would lead one to expect a spectral distribution of reflected energy that would peak up toward the low Doppler frequencies, in contrast to the broad, flat characteristics of the observed clutter-related noise.

(U) {(S)} There is no doubt that the effects described in this section do exist. Investigations have aimed at using such effects for the radar identification of man-made objects. (42) Whether the effects are quantitatively consistent with being the source of the clutter-related noise observed with the AN/FPS-95 is, however, not known.

(U) {(S)} In order to test the hypothesis that clutter-related noise was generated by earth-surface effects, such as those just described, the Land/Sea Experiment was performed. This experiment was designed to identify the existence, if any, of persistent differences in the clutter-related noise levels from geographically separate areas of the AN/FPS-95 coverage. In particular, the experiment was designed to include a comparison of land and sea areas, since such a comparison should reveal large differences in clutter-related noise if the clutter-related noise was generated by man-made artifacts. The results of the experiment (see Appendix) were consistent with the theory that little, if any, of the clutter-related noise was generated by reflections from the sea areas, when compared with that from the land areas. In contrast, the clutter levels returned from the sea areas were roughly similar in power to those from the land areas. These two facts support the hypothesis that the clutter-related noise is generated by some reflection mechanisms operating within the land areas of the AN/FPS-95 coverage, and is not caused by spectral spreading of the radar energy occurring either before or after reflection at the land or sea surface.

Multihop Effects

(U) {(S)} It is known that, as expected, the effect of a rising or falling ionospheric layer is to shift the frequency of radiation reflected from the layer. It

TABLE 8. *Propagation medium effects.* (*Table unclassified.*)

Postulated Cause \ Observation	One-Way OTH Path Tests	Sporadic E/F-Layer Comparison	Transmitter Power Reduction Test	Aurora Measurements	Land/Sea Comparison
F-Layer Vertical Motion and Waves	√				√
E-Layer and Sporadic-E Vertical Motion and Waves		√			√
Ionospheric Modification and Heating	√		√		√
Meteor-Induced Power Flow Modulation	√				√
Aurora-Induced Power Flow Modulation	√			√	√

was therefore suggested that the radar energy arriving back at the receiver, after many such reflections from multihop propagation modes, might be a cause of clutter-related noise.

(U) ~~(S)~~ One reason that this would seem to be unlikely is that such multihop returns would not generally coincide in range with that of the observed clutter-related noise, which is always approximately coincident with the ground clutter. Another reason concerns the fact that the observed single-hop Doppler shift due to rising or falling ionospheric layers is usually less than 1 Hz. Since the amplitudes of the returns from successively higher orders of hop would generally be attenuated, one would expect the corresponding spectrum to fall off sharply with frequency. It would also be rare to encounter the particular mix of rising and falling layers necessary to account for a symmetrical spectrum. From this reasoning, it appears unlikely that multihop effects could explain clutter-related noise: This conclusion is strengthened by the low PRF observations performed during the short-range noise experiment,[34] wherein clutter-related noise was observed during radar operation at a PRF of 10 Hz.

PROPAGATION MEDIUM EFFECTS

(U) The spectra of high-frequency radar signals could be corrupted by a number of mechanisms in passing from the radar antenna over the horizon to the earth's surface. It is the dual purpose of this section first to list the various phenomena that have been postulated as possible mechanisms for such spectral corruption and then to review the evidence for and against each case as the cause of observed clutter-related noise. Here we consider only *transmission* effects; *reflection* effects are dealt with in the preceding section.

(U) ~~(S)~~ The matrix of Table 8 lists at the left specific phenomena that have been put forward as possible causes in the transmission medium for clutter-related noise. Across the top are the names of various experiments that were performed to confirm or deny one or more of the causes. Check marks signify which experiments relate to the various postulated causes. The method here will be to consider each phenomenon in turn and to review for each the relevant experimental evidence that was generated in the attempts to find and eliminate the cause of the noise.

F-Layer Vertical Motion and Waves

(U) ~~(S-NF)~~ The experiments which bear on the F-layer of the ionosphere as the unique cause of clutter-related noise are the One-Way Path Tests,[35,36] the Sporadic E-Layer/F-Layer Experiment,[37] and the Land/Sea Test. (33) These tests are described earlier in this section.

(U) {(S-NF)} One-Way Path Tests, which consisted of transmissions both ways between England and the Eastern Mediterranean via F-layer refraction, showed no contamination of spectra induced by the medium down to the dynamic-range limits of the measuring equipment to excess of 80 dB. About the only ionospheric effects noted were simple spectral shifts of 1 to 2 HZ caused by ionospheric vertical motion.

(U) {(S)} In the E-Layer/F-Layer test, ground clutter returns via one-hop sporadic-E and one-hop F-layer propagation modes were observed and analyzed. Clutter-related noise was observed on both sporadic E- and F-mode returns. The characters of the noise and the clutter-to-clutter-related noise ratios in the two cases were essentially the same.

(U) {(S)} Finally, the result of the Land/Sea Backscatter Test showed that the clutter-related noise associated with the clutter return from sea surfaces was significantly less than that associated with clutter returns from land surfaces at the same range and in adjacent beams. A mechanism in the F-region that can create the spectral contamination at different levels relative to the clutter for land and sea reflection surfaces is difficult to conceive.

E-Layer and Sporadic-E Vertical Motion and Waves

(U) {(S)} Remarks along the lines of those given for the F-layer above relate also to the E-layer as the possible unique source of the contamination (that is, clutter-related noise) of the clutter spectrum when the clutter return passes through or is refracted by the E-layer of the ionosphere. One significant point is that clutter-related noise was always observed, even at night when the E-layer did not exist, whenever propagation support was strong enough to raise the clutter returns to 70 dB or so above natural background noise. And again, the Land/Sea Test (33) seems to rule out the propagation medium ns a whole as the source of clutter related noise.

Ionospheric Modification and Heating

(U) {(S-NF)} It has been conjectured that the observed clutter-related noise could result from the heating of the ionosphere caused by high power of the transmitted signal. Ionospheric heating calculations, (20,43,44) the Transmitter Power Reduction Test, (25) and the One-Way Path Tests (35,36) relate to this possible cause, as do the Land/Sea Tests. (33)

(U) {(S)} Calculations predict (*1*) that, at the power levels associated with the AN/FPS-95 and for low-angle transmitted rays, caustics will occur at approximately E-region heights following F-layer refraction, (*2*) that the ionosphere will be heated in the region of the caustic, and (*3*) that the, spectrum of the radar signal will be distorted. The distortion, calculations show, should result in an asymmetric broadening of the central line of the radar signal spectrum on the recede-Doppler side. The amount of the broadening predicted is about 2 HZ. Ionospheric heating would *not*, according to calculations, account for the approximately flat amplitude excess noise (that is, the so-called clutter-related noise) that fills the entire unambiguous Doppler-frequency region.

(U) {(S)} Further, any effect caused by ionospheric heating should change with power level, and changes in the level of clutter-related noise with respect to that of the clutter or in the character of clutter-related noise (for example, the spectral shape) with transmitter power level were never observed, either in ordinary day-to-day operation or in the Transmitter Power Reduction Tests. As before, the results of the Land/Sea Tests imply that clutter-related noise is not caused by ionospheric heating or, indeed, by any effect in the propagation medium.

Meteor-Induced Power-Flow Modulation

(U) {(S)} Some attempts have been made to relate both backscattering and forward scattering from the so-called "meteor belt" located about 100 km above the earth with the observed clutter-related noise. All over-the-horizon backscatter signals pass through the meteor belt four times, and the forward power flow of the signal conceivably could be modulated by interaction with meteors to create the clutter-related noise. The experiments relevant to possible meteor-induced power flow modulation as a cause of clutter-related noise are the One-Way Path Test (35,36) and the Land/Sea Test. (33)

(U) {(S)} In regard to the One-Way Path Test, none of the results supported the hypothesis that the meteor belt corrupted in a measurable way the spectrum of the forward-scattered signal. During reception of the AN/FPS–95 signal in the Eastern Mediterranean, we looked for meteor-belt-induced forward scatter by slewing the range gate ahead of and behind the main received radar pulse. Results were inconclusive, perhaps because of a lack of adequate isolation of the gate. But the spectrum of the received direct signal was not measurably corrupted in any way. As before, the Land/Sea Test results imply that the cause of clutter-related noise is not in the transmission medium.

Aurora Power Flow-Modulation

(U) ~~(S)~~ The question here is whether the cause of the observed clutter-related noise could be a modulation of the signal resulting from interaction with aurora as the signal passed through the propagation medium.

(U) ~~(S)~~ To cause spread-frequency noise (that is, noise resembling clutter-related noise) to be present in range intervals containing returns reflected from the earth's surface, either the main signal would have to be corrupted in passing through aurora-disturbed regions or the corruption would have to be impressed upon non-main-path signal components (that is, transmissions of the signal over paths containing aurora in the antenna sidelobe direction, and so on) that arrived back at the radar receiver at times corresponding to those of the arrival of the main-path clutter returns. For the former—corruption of the main signal by passage through auroral regions—transmission would have to be along certain beams, namely, the more northerly beams, and at times when aurora was present. One would then expect the clutter-related noise to occur in northerly beams only when aurora was present. But clutter-related noise was present with clutter returns from northerly beams whether aurora was present or not.[12] In fact, clutter-related noise was observed in returns via all beams, including southerly beams, whether aurora was present in the north or not. In regard to the conjecture that aurora-induced noise entered through the sidelobes of the antenna, studies[12] that analyzed the return in each beam as a function of time, range, and magnetic activity made it possible to distinguish and categorize auroral clutter. The studies also found, at times and for some beams, that auroral clutter could increase the noise level in the range bins containing ground clutter, but that *mostly* it would not.[12]

FEASIBILITY OF ELECTRONIC COUNTER MEASURES AS THE SOURCE OF EXCESS NOISE

(U) ~~(S)~~ In the absence of any convincing conventional explanation for the clutter-related noise, some speculated that the noise could have been generated deliberately. After all, the AN/FPS–95 was engaged in a surveillance of the Soviet Union and the Soviet-Bloc countries, a function that could have been deeply resented. Perhaps this resentment provoked countermeasures to reduce the radar's effectiveness and ultimately remove it from the scene. Admittedly, the notion seems "far fetched"; however, it is not easily disposed of and remains a possible explanation for the noise. In this section, we explore this possibility and describe how it could have been done.

(U) ~~(S)~~ If countermeasures were employed, they were not of the conventional jamming type, because jamming in the ordinary sense would have been observed by the site personnel. Furthermore, such jamming would have both violated international agreements and incurred severe criticism. But a jamming technique not easily recognized as jamming might be a distinct possibility. Granted that the notion of "covert jamming" seems even more ridiculous, it is, however, not without precedent. There is a technique referred to by some as "Villard's Disclosure" that provides a basis for covert jamming in OTH systems.* Over-the-horizon radars generally have large transmitting antennas and high-power transmitters, which combine to produce large power densities in the target coverage area. The actual return from the targets of interest is quite small compared with the incoming radiation and its scattered components from ground clutter. These target returns are detectable at the radar because OTH radar has a large receiving aperture; in the target coverage area, however, the target returns tend to be masked or covered by the large incoming and ground-scattered signals. In other locations, it is also difficult to discern the signals reflected from the target because of the large clutter return that covers the signal. These clutter returns are also present at the radar, but are removed by compli-

*(U) Probably because the technique was disclosed by O. G. Villard, Jr., many years ago, but the authors do not have a reference to support this conjecture.

cated Doppler processing equipment that separates target returns from clutter returns on the basis of their motion. Suppose, then, that an adversary generated a signal in the target area that is proportional to the radar illumination and somewhat larger than the returns from a legitimate target, but much smaller than the returns from clutter. Further, suppose that this signal spreads across the spectrum to fill both the unambiguous Doppler band and the illuminated range interval. The world at large would never see this jamming signal because, as a rule, ordinary antennas are small and no equipment is available to separate the jamming from the covering clutter return. At the OTH radar, though, the signal would not only be visible, but would also mask the targets of interest. It would, in fact, exhibit all the properties of clutter-related noise, triggering in turn a some what predictable chain of events. The first reaction would be that, since the clutter return was not fully cancelled, something must be wrong with the radar. If we found the radar to be fault-free, we would blame the ionosphere. If we exonerated the ionosphere, we would blame the clutter. In the end, we would lose patience and summarily cancel the program without ever discovering the cause. This is indeed covert jamming.

(U) {(S)} At this point, we will briefly describe how this jamming technique could be implemented. There are of course many ways, but we describe only one.

(U) {(S)} The radar coverage of the AN/FPS-95 was a region spanning approximately 90 deg In azimuth and from 500 to 2,000 nmi in range from Orford Ness, England. Select 15 sites in this region, anywhere in azimuth but separated by 100 nmi in range. At each site, install a linear array of 16 monopoles with a backscreen boresighted on Orford Ness. (Such an antenna has been built at MITRE for a cost of about $25,000, and it has a gain of 25 dB.) Each site would be equipped to recognize the AN/FPS-95 signal by its power, pulse width, PRF, and direction of arrival. (One element of the array could be used for a sidelobe cancellation device.) Each site would also be provided with a linear transmitter that would, upon the reception of the AN/FPS-95 signal, repeat its signal offset in frequency and in every Doppler cell and in every range cell for 100 nmi trailing the range of the site. Each site that was illuminated would in turn fill its portion of the total area illuminated by the AN/FPS-95. The 100-nmi uncertainty at the beginning and end would hardly be noticed. Each site would sense its being either in a sidelobe or the main beam of the AN/FPS-95 and adjust the level of its transmitted signal to exceed that of legitimate radar targets by 10 dB, taking into account sidelobe/main-beam receiving gains of the AN/FPS-95. By and large (12 out of 13 times), the site would be working into the AN/FPS-95 sidelobes, but when the main beam happened on the site, it would attenuate its normal transmission by about 20 dB. The power requirement can be determined as follows: let

S = signal power received from a target,

J = signal power received from a jamming site per resolution cell,

P = average power of the radar,

j = average power of the jammer per resolution cell,

G = gain of the radar antenna,

g = gain of the jammer antenna,

A = receiving aperture of the radar,

s = sidelobe level of the radar antenna below the main-beam gain,

X = radar cross section of the target ,

R = range to the target from the radar,

r = range to the jammer from the radar,

L = radar propagation losses, and

l = jammer propagation losses.

Then $$s = \frac{P\ G\ X\ A}{(4\pi R^2 L)^2} \qquad (2)$$

and $$J = \frac{j\ g\ A\ s}{4\pi r^2 l}z \qquad (3)$$

If $$J = 10\ S \qquad (4)$$

then from Eqs. (2) and (3),

$$j = \frac{10\ P\ G\ X\ r^2 l}{4\pi R^4 L^2 g\ s} \qquad (5)$$

Now if

P = 300 kW,

G = 25 dB,

g = 25 dB,

s = 20 dB,

R = 500 nmi,

r = 500 nmi,

$$\sigma = 100 \text{ m}^2,$$
$$L = 10 \text{ dB, and}$$
$$l = 10 \text{ dB},$$

then $\bar{p}=2.78\times10^{-4}$ watts/resolution cell.

(U) ~~(S)~~ Since the shortest pulse used on the AN/FPS-95 was 250 μsec long, corresponding to 20 nmi in range, each jammer must fill no more than five range cells. Since trailing cells require less power than the first cell, the power requirement due to range cells is less than five times the power requirement for the first cell. The highest PRF of the AN/FPS-95 was 160 Hz, and with 10 sec of integration, there are no more than 1,600 Doppler resolution cells. Consequently, there are less than 8,000 resolution cells in total, and the worst-case jammer at 500 nmi would require less than 2.22 watts. A site at 2,000 nmi would require 1/256 of this power. In either case, the jammer power requirements are quite small.

(U) ~~(S)~~ We are forced to conclude that the jamming technique is quite feasible, and it is not clear that the experiments conducted at the AN/FPS-95 would have discovered the jamming had it occurred. If experiments confirming or denying the possibility had been conducted, they would have perhaps resolved the issue. They were not conducted.

SUMMARY AND CONCLUSIONS

(U) ~~(S)~~ The AN/FPS-95 OTH radar built by the U.S. Air Force on the North Sea Coast of England in the late 1960's was plagued by noise that severely limited subclutter visibility and, thus, seriously impaired the detection performance of the radar. All-out attempts to locate and correct the source of the noise in the relatively brief time allotted in late 1972 and early 1973 were unsuccessful: The source was not found. Subsequently, the program was terminated abruptly on June 30, 1973, after which the radar was dismantled and its components removed from the site.

(U) ~~(S)~~ A host of tests were performed on the radar equipment to see if it contained the source of the noise. In the end, the equipment was exonerated; furnished by RCA Corp., Moorestown, N.J., it was generally of high quality and was judged as almost certainly *not* the source of the clutter-related noise.

(U) ~~(S)~~ Tests on the environment external to the radar seem to eliminate as causes of the noise all effects except what we have called earth-reflection effects. While the results of the Land/Sea Test, which explored the earth-reflection effects, are generally consistent with the hypothesis that clutter-related noise is present in returns from land surfaces and not present in returns from sea surfaces, the evidence is too limited, both in time and in regions examined, to be considered conclusive.

(U) ~~(S)~~ As this paper suggests, a few inexpensive, simple, repeater-type jammers with a few watts of power output each, distributed over the radar coverage zone, conceivably could have produced effects like those identified in the paper as clutter-related noise. No tests performed at the radar either confirm or deny the hypothesis that jamming caused the clutter-related noise.

(U) ~~(S)~~ The strange legacy of the AN/FPS-95 is the enigma surrounding the clutter-related noise. In all the time since the program terminated, the radar community—even including some OTH radar specialists—does not seem to have assimilated either the nature of the difficulty that beset the AN/FPS-95 or the details of the program that was mounted to try to find the cause. There seems to be a feeling that the Cobra Mist experience was anomalous and that the affliction will not recur. The authors would caution against such a view.

(U) ~~(S-NF)~~ The AN/FPS-95 experience may indicate that natural effects of some kind limit the subclutter visibility achievable in high-frequency OTH radars to about 60 to 70 dB. The AN/FPS-95 was the first OTH radar with enough power routinely to generate clutter returns 80 to 90 dB above external CCIR noise levels. Therefore, it is perhaps the first OTH radar to be afflicted routinely with clutter-related noise. But not the only one: During the Cobra Mist tests in 1973, members of the Scientific Assessment Committee visited another OTH radar site, bringing back data records that clearly showed noise resembling clutter-related noise in range bins containing ground-clutter returns.[7] So, at least in 1973, clutter-related noise was observed at another OTH radar.

(U) ~~(S)~~ If the cause of clutter-related noise is an area effect—and some believe that it is—it can be overcome in design by giving an OTH radar adequate spatial resolution, so that the returns from objects that the radar is to detect appear at levels well above the AN/FPS-95 observed clutter related noise level. One might require, for example, that the spatial resolution of an OTH radar be such that the amplitude of returns from targets of interest be within about 40 to 50 dB of the earth clutter return. Moreover, regarding countermeasures, designers of future OTH radars, conceived to overlook the land area of an adversary, should remember that an OTH radar like the AN/FPS-95 would be relatively easy to jam and that the jamming would be difficult to detect.

(U) {(S)} It is the hope of the authors that this paper will stimulate informed discussion and debate about the cause, or causes, of clutter-related noise. The clutter-related noise anomaly should be pursued: Resolution of such anomalies almost always is accompanied by a significant advance in knowledge and understanding.

APPENDIX: THE LAND/SEA EXPERIMENT (33)

(U) {(S)} The objective of this experiment was to determine whether or not there were persistent differences between the levels of clutter-related noise within a range-azimuth resolution cell as a function of the geographic position of the cell. In particular, it was desired to compare those cells located over land with those over water.

(U) {(S)} Conceptually, the ideal way to carry out the comparison would be to hold all the other relevant radar parameters constant during the measurement and to varying the geographical area within the resolution cell. Since this was obviously impossible, the experiment was designed to minimize, as far as possible, the differences in these parameters while alternating between the two measurements. This was achieved by comparing only pairs of resolution cells that were close together, that is, at the same ranges, but in adjacent azimuth beam positions, It was judged that this method would be superior to that of comparing adjacent range resolution cells within one beam, because the noise was known to be highly range dependent and also because the absolute position in range of the cells was subject to some uncertainty because of ionospheric layer height uncertainties. As the two resolution cells were at the same range and adjacent, the respective radar propagation paths would have very similar vertical profiles (assuming a well-behaved ionosphere), and the take-off angles at the antenna - and by implication, the relative gains - would likewise be similar. The effect of temporal variations in the clutter-related noise during the cell-pair comparisons was minimized by making the second cell measurement immediately after the first and then averaging a large number of such measurements. Possible differences between the antenna gains at adjacent azimuth beam positions would be revealed by a comparison of surface-clutter returns in those areas where the two beams both straddled areas of similar surface, that is, both land or both sea. It was hoped that gain differences would be small, since five of the six antenna strings were common between adjacent beams. Many measurements were spread throughout the diurnal cycle. This had the incidental effect of requiring a range of radar operating frequency to accommodate different ionospheric conditions, which consequently produced differences in the take-off angles of the radiation from the antenna. It should be emphasized, however, that during any single comparison measurement between adjacent resolution cells, the frequency was held constant. The diversity in frequency and elevation take-off angle was not considered detrimental, since it would tend to smear out any possible (although unlikely) antenna effects that might conceivably generate clutter-related noise over a very small range of elevation angles more in one beam than in the adjacent beam. Since this effect would have resulted in a persistent variation of clutter-related noise as a function of azimuth and range, it could have led to a misinterpretation of the experimental results.

Area of Observation

(U) {(S)} The area selected for observation was bounded by beams 9 and 13, inclusively, and by ground ranges of 1,000 and 1,500 nmi (Fig. 17). It was chosen mainly for the reason that it contained a large portion of the Black Sea and had the requisite land/sea boundaries between azimuth beam positions. Additionally, the area's terrain features and industrialization levels varied widely. Another important consideration was that the chosen radar ranges should not allow single-hop E-layer propagation modes, with consequent confusion between these modes and the normal one-hop F-modes.

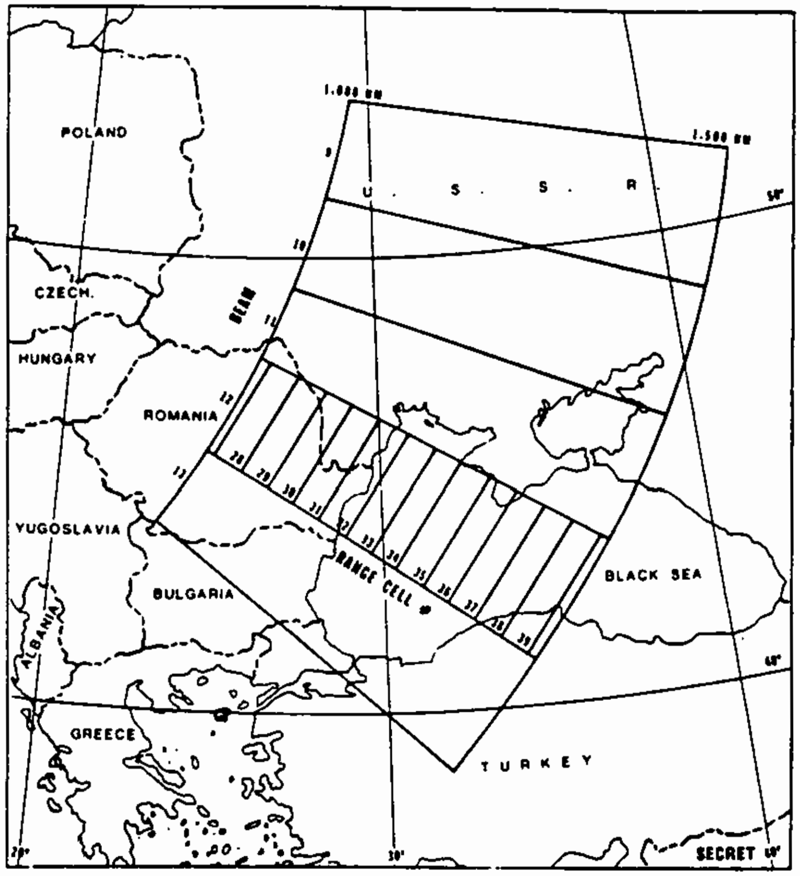

Figure 17. The geographical coverage chosen for the Land/Sea Test. (~~Figure classified Secret.~~)(U)

The beam positions on Fig. 17 correspond to the nominal azimuth directions of the AN/FPS–95 antenna structure. The radial lines indicate the nominal one-way half-power bearings of each beam. Measurements of the actual antenna patterns[45] revealed that the beam positions squinted inward, so that the high-number beams were actually pointing several degrees north of their nominal positions. This fact is important in the interpretation of the experimental data. The range-resolution cells drawn in beam 12 are each 40 nmi long. Reference to these cells is by the numbers indicated in the figure.

Operating Parameters and Procedures

(U) During data gathering, the AN/FPS–95 was operated using the following parameters:

Frequency: Variable
Pulse length: 500 μsec
Pulse shape: Cosine-squared
PRF: 40 pulses/sec
Antenna polarization: Horizontal
Beam numbers: 13, 12, 11, 10, and 9

(U) For each run, the data were recorded first in beam 13 for 2 min. Beam 12 was then similarly treated, and so on down to beam 9. The 10 min of data thus recorded on magnetic tape were all taken using a single radar frequency. Subsequent 10-min runs would not necessarily be at the same frequency. Over the course of the experiment, approximately 8 hr of data were recorded and analyzed.

Data Analysis

(U)~~(S)~~ A full description of the signal and data analysis is beyond the scope of this paper, and the interested reader is referred to Ref. 33. Briefly, however, for each range cell the 2-min sequence of signal returns was divided into batches of 3.2-sec duration (128 samples) and submitted to an off-line spectral analysis. This permitted the ground- or sea-clutter returns, which are located in the vicinity of zero Doppler shift, to be separated from the clutter-related noise. Measurement of total clutter power was made in a Doppler band extending from +5 Hz to −5 Hz. Clutter-related

Table 9. *Median clutter-related noise power. (33) {(Table classified Secret)}* (U)

Beam Number	Range Cell Number					
	29	30	31	32	33	34
9		L 35	L 44	L 48	L 34	L 35
10		65 L 53	56 L 52	52 L 40	66 L 48	65 L 56
11	L 45	47 L 47	48 L 58	60 L 81	52 L 87	44 L 82
12	55 L	53 L	42 L	19 S 40	13 S 43	18 S
13				80 L	57 S	

Table 10. *Clutter power. (33) {(Table classified Secret)}* (U)

Beam Number	Range Cell Number					
	29	30	31	32	33	34
9		L 42	L 47	L 54	L 50	L 48
10		58 L 50	53 L 58	46 L 55	50 L 43	52 L 53
11	L 39	50 L 50	42 L 47	45 L 38	57 L 48	47 L 42
12	61 L	50 L	53 L	62 S 48	52 S 55	58 S
13				52 L	45 S	

noise was measured in a frequency band extending from +5 Hz to +15 Hz. The measurements of ground or sea clutter and of the clutter-related noise that were thus produced for all of the 3.2-sec intervals within a 2-min recording were averaged to obtain smoothed estimates. These estimates were then paired with similar estimates obtained from the same range cell in the adjacent azimuth beam, which were obtained from measurements made 2 min after those of the first beam. From these pairs was calculated the fraction of the total, clutter or clutter-related noise in each pair of resolution cells attributable to each member of the azimuth beam pair. The fractions thus calculated were further averaged over all of the valid 2-min recordings. The number of fractions thus averaged varied from cell-pair to cell-pair and between clutter and clutter-related noise due to the application of data-validation algorithms. After rejecting invalid data, the number of fractions averaged ranged from a low of 18 to a high of 46, each representing 2 min of raw recorded data.

Results

(U) {(S)} The results of the experiment are tabulated in Tables 9 and 10 for the clutter-related noise and clutter, respectively. The interpretation of these tables is best explained by means of an example. Referring to Table 9, the letters L and S indicate whether a particular resolution cell was predominantly on land or on sea. Consider range cell 32 and the line separating beam 11 from beam 12. The numbers 81 and 19 will be found straddling this line. This means that the noise powers observed in beam 11, range cell 32, and in beam 12, range cell 32 were measured to be in the ratio of 81 to 19.

Interpretation of Results

(U) {(S)} Examination of Fig. 17 shows that two of the resolution cells in beam 12 (cells 33 and 34) are completely over the water out to and beyond the half-power one-way beamwidth points. If it is assumed that the clutter-related noise is returned only from land areas, then an integration of the two-way beam pattern across, and well beyond, the half-power one-way beamwidth would produce the conclusion that the ratios of clutter-related noise in beam 11, range cells 33 and 34, to that in beam 12, range cells 33 and 34, should be much larger than indicated in Table 9. However, as mentioned previously, the actual high-number beam positions, as measured during limited airborne antenna pattern calibrations, were skewed around toward the north by amounts ranging roughly from 3 deg to 7 deg. With such beam shifts, the land on the northern side of the Black Sea would be positioned in the skirts of beam 12, thereby increasing the amount of clutter-related noise received in that beam. A numerical integration of the two-way antenna pattern for various assumed beam skews shows the following results for the expected ratios of clutter-related noise in beam 11 to that in beam 12 at the ranges of range cells 33 and 34.

Assumed Northerly Skew (deg)	*CRN Ratio*
0	28:1
3	7:1
5	2:1

(U) ~~(S)~~ These clutter-related noise ratios are seen to be not inconsistent with the ratios of 87:13 and 82:18 from Table 9, assuming existing beam skews of approximately 3 to 4 deg, which is within the range of the measured beam skews.

(U) ~~(S)~~ From the preceding arguments, it appears that the experimental measurements of clutter-related noise are fully consistent with the hypothesis that little, if any, clutter-related noise is returned from resolution cells corresponding to sea areas when compared with clutter-related noise returned from land cells. As Table 9 shows, the clutter-related noise variation between either adjacent pairs of land cells or an adjacent sea cell pair is generally much smaller than that observed at land/sea boundaries. The data in Table 10 for clutter returns are particularly interesting when compared with the clutter-related noise data in Table 9, for they show that at the land/sea boundaries, and unlike the clutter-related noise behavior, the clutter levels do not change appreciably. These facts do not support theories of clutter-related noise generation that propose that the radar energy is modulated during propagation to form clutter-related noise either before or after being scattered back from the land or sea surface. If such were the case, there would be little difference between the clutter-related noise returned from the land areas and that from adjacent sea areas.

ACKNOWLEDGMENTS

(U) The authors are grateful to the following of their MITRE colleagues for assistance in the preparation of this paper: William K. Talley, Adolph Fejfar, Nicholas M. Tomljanovich, Fred G. Benkley, and Dominic J. Marino. Special thanks are due Jeanne R. Rainoldi, who did much to make the manuscript more readable. Bobbi Statkus, who produced the typewritten text, and Mary Mills, who prepared the tables and illustrations for reproduction, also deserve our thanks. We are indebted to Charles M. Brindley and Sheldon M. Paskow of RCA Corp., Moorestown, N.J. and to John Schneider of the U.S. Air Force, Rome Air Development Center, Griffiss Air Force Base, N.Y. Finally, it is a pleasure to thank Col. Erlind Royer, U.S. Air Force Electronic Systems Division, Hanscom Air Force Base, Mass. for agreeing to sponsor the paper.

REFERENCES

1. *AN/FPS-95 Research and Development Program*, Volume I: "Overview"; Volume II: "Final Technical Report, Naval Research Laboratory," (Part A, General; Part B, Missile Detection; Part C, Surface Wave Investigation; Part D, Doppler Resolution; Part E, Frequency Diversity; Part F, Synoptic Measurements; Part G, Long-Path Propagation Effects; Part H, Meteor Effects; Part I, Performance Prediction Investigation; Part J, Noise/Interference Environment; Part K, Radar Signal Processing Computer Program); Volume III: "Final Technical Report, The MITRE Corp.," (Part A, General; Part B, Auroral/Environmental Effects; Part C, Range and Azimuth Calibration; Part D, Track-While-Scan Development; Part E, Land/Sea Subclutter Visibility; Part F, Comparative Antenna Subclutter Visibility Measurements; Part G, Antenna-Induced Noise Measurements; Part H, Interactive Display Development; Part I, Design of Noise Measurement Instrumentation; Part J, Signal Processing Program System Computer Program); ESD TR-73-270, U.S. Air Force Electronic Systems Division, L. G. Hanscom Field, Mass., April 1974 (Secret).
2. F. H. Utley et al., "The Utility of an OTH Radar in the Detection of a Large-Scale Air Attack on the CONUS," *Proc. OHD Tech. Rev. Mtg. 11–12 Dec. 1969*, Vol. II, Experimental Measurements, page 1, Stanford Research Institute, Menlo Park, Calif. (Secret).
3. J. R. Davis et al., "Ionospheric Earth Backscatter and Precision Ray-Tracing Applied to the Analysis of Over-the-Horizon Rocket Launch Signatures," *Proc. OHD Tech. Rev.*

Mtg 23-25 Oct. 1968, Vol. II, page 47, Stanford Research Institute, Menlo Park, Calif. (Secret).

4. *Experimental Plan for COBRA MIST Design Verification Program*, MTR-932, COBRA MIST Working Group, E.L. Key, Chairman, The MITRE Corp., Bedford, Mass., Aug. 15, 1969 (Secret).

5. E.L. Key et al., *Report of Technical Advisory Committee Meeting 14-16 November 1972*, Control No. 5200-B0166, The MITRE Corp., Bedford, Mass., Nov. 28, 1972 (Secret/Noforn except U.K.).

6. M. Balser et al., _Test Program - Scientific Assessment Committee_, Control ESD-9346, Air Force Electronic Systems Division, L.G. Hanscom Field, Mass., Jan. 29, 1973 (Secret/Noforn except U.K.).

7. M. Balser et al., *The Report of the U.S.-U.K. COBRA MIST Scientific Assessment Committee*, Control ESD-9639, Air Force Electronic Systems Division, L. G. Hanscom Field, Mass., May 1, 1973 (Secret/Noforn except U.K.).

8. *Radar Set An/FPS-95 Summary Information*, Parts I, II, and III, MO-991, RCA Corp., Moorestown, N.J., July 1968 (Secret/Noforn except U.K.).

9. A. Fejfar, *Analysis of System Performance AN/FPS-95*, MTR-2127, The MITRE Corp., Bedford, Mass., Sept. 10, 1971 (Secret).

10. A.F. Barghausen et al., *Predicting Long-Term Operational Parameters of High-Frequency Sky-Wave Telecommunications Systems*, ERL-110-ITS-78, Institute for Telecommunications Sciences, Boulder, Colo., May 1969.

11. J.F. Thomason, *Final Technical Report on the AN/FPS-95 Research and Development*, Vol. II, Part B, "Missile Detection," NRL-2762, Naval Research Laboratory, Washington, D.C., May 1974 (Secret).

12. A. Fejfar, *AN/FPS-95 Research and Development Program (Final Technical Report, MITRE, Auroral Environmental Effects)*, MTR-2777, The MITRE Corp., Bedford, Mass., July 1974 (Secret).

13. J.R. Earlam, *AN/FPS-95 Research and Development Program, Final Technical Report, MITRE, Track-While-Scan Development*, Vols. I and II, MTR-2754, The MITRE Corp., Bedford, Mass., July 1974 (Secret).

14. B.D. Perry, *Special Information on High-Frequency Radar - Final Report on Experiment 506*, MTR-2565, The MITRE Corp., Bedford, Mass., August 1974 (Secret).

15. *World Distribution and Characteristics of Atmospheric Radio Noise*, International Radio Consultive Committee (CCIR), Rpt. 322, International Telecommunication Union, Geneva, Switzerland, 1963.

16. R.G. Curtis and S.C. Vorenberg, *AN/FPS-95 Research and Development Program, Final Technical Report, MITRE, Interactive Display Development*, MTR-2752, The MITRE Corp., Bedford , Mass., July 1974 (Secret).

17. R.I. Millar, *Effects of Range-Related Noise on System Performance*, Rpt. D81-0B-372, The MITRE Corp., Bedford, Mass., Nov. 21, 1972 (Secret) .

18. E.H. Bensley, *AN/FPS-95 Research and Development Program, Final Technical Report, MITRE, Signal Processing Program System*, Vols. I through VI, MTR-2589, The MITRE Corp., Bedford, Mass., July 1974 (Secret).

19. P.B. Bentley, *An Evaluation of the AN/FPS-95 Receiver, Transmitter, and RF Hardware*, Proj. 2415, Stanford Research Institute, Menlo Park, Calif., March 5, 1973 (Secret/Noforn except U.K.).

20. A.S. Robinson et al., *Initial Plan of the Ad Hoc Radar Propagation Committee, Rpt. MA-002383*, RCA Corp., Moorestown, N.J., Dec. 1, 1972 (Secret/Noforn except U.K.).

21. F.G. Benkley, *Noise Sources in the AN/FPS-95*, WP-20622, The MITRE Corp., Bedford, Mass., Feb. 27, 1976 (Secret).

22. F.G. Benkley, *Intermodulation Tests of AN/FPS-95 Receiving System*, D81-0B-252, The MITRE Corp., Bedford, Mass., May 24, 1972 (Secret/Noforn except U.K.).

23. F.G. Benkley, *Cross-Modulation in OTH Systems*, D81-0B-253, The MITRE Corp., Bedford, Mass., May 24, 1972 (Secret/Noforn except U.K.).

24. F.G. Benkley, *Environmental Data Obtained on 28, 29, 30 December 1971*, D81-0B-173, The MITRE Corp., Bedford, Mass., Jan. 10, 1972 (Secret/Noforn except U.K.).

25. R.I. Millar, *Investigation of Range-related noise Phenomenon*, D81-0B- 312, The MITRE Corp., Bedford, Mass., Sept. 20, 1972 (Secret/Noforn except U.K.).

26. F. G. Benkley, *AN/FPS-95 Research and Development Program, Final Technical Report, MITRE, Antenna-Induced Noise Measurements*, MTR-2753, The MITRE Corp., Bedford, Mass., March 1975 (Secret).
27. R. P. Rafuse, *Rationale for the Design of a Wide-Spaced 1/6-Scale Model 9 Element Yagi Antenna for 141 MHz*, RATM-73-4, Rafuse Associates, Harvard, Mass., Jan. 18, 1973.
28. F. G. Benkley, *AN/FPS-95 Tests Using Repeater*, D81-0B-379, The MITRE Corp., Bedford, Mass., Nov. 29, 1972 (Secret/Noforn except U.K.).
29. R. I. Millar, *Measurements of AN/FPS-95 Subclutter Visibility Employing an Auxiliary Antenna*, MTR-2720, The MITRE Corp., Bedford, Mass., February 1974 (Secret).
30. C. J. Beanland, The MITRE Corp., Bedford, Mass., private communication, April 1973 (Secret).
31. P. E. V. Shannon, *Final Technical Report on the AN/FPS-95 Research and Development Program, Vol II, Part D, Synoptic Measurements*, Naval Research Laboratory, Washington, D.C., February 1974 (Secret).
32. F. G. Benkley, *Comparison of Range-Related Noise in Different Time Periods*, Memo. 5200-R0260, The MITRE Corp., Bedford, Mass., May 7, 1973 (Secret).
33. R. H. Sear, *Land/Sea Subclutter Visibility*, MTR-2751, The MITRE Corp., Bedford, Mass., August 1974 (Secret).
34. J. F. Thomason, *Final Technical Report on the AN/FPS-95 Research and Development Program, Vol. II, Part E, Noise/Interference Environment*, Naval Research Laboratory, Washington, D.C., January 1974 (Secret).
35. D. G. Trizna, *Final Technical Report on the AN/FPS-95 Research and Development Program, Vol. II, Part F, Long-Path One-Way Propagation Effects*, Memo. Rpt. 2721, Naval Research Laboratory, Washington, D.C., February 1974 (Secret).
36. R. B. Wall, *Results of Measurements of COBRA MIST and . . . Signals*, Control 5200-R0246, Memo. D81-0B-470, The MITRE Corp., Bedford, Mass., March 22, 1973 (Secret/Noforn except U.K.).
37. A. Fejfar, *A Comparison of Simultaneous Sporadic E and F Data*, Appendix D to Ref. 31 (Appendix classified Secret).
38. L. A. Manning and V. R. Eshleman, "Meteors in the Ionosphere," *Proc. IRE XLVII*, 186 (1959).
39. E. D. R. Shearman, "The Technique of Ionospheric Investigation Using Ground Backscatter," *Proc. IEE 103B*, 210 (1955).
40. F. H. Utley et al., *Meteors, Their Impact on OTH Radar Systems*, Radar Techniques Branch, Naval Research Laboratory, Washington, D.C., March 1973 (Secret).
41. *Polar Cap III Program Report*, Electronic Systems Division, Air Force Systems Command, Hanscom Air Force Base, Bedford, Mass., Oct. 31, 1974 (Secret).
42. R. G. Newburgh, *Basic Investigations of the RADAM Effect*, RADC-TR-78-151, Rome Air Development Center, Air Force Systems Command, Griffiss Air Force Base, N.Y., June 1978.
43. N. M. Tomljanovich, *Ionospheric Heating Effects on Oblique Ray Propagation*, briefing report, The MITRE Corp., Bedford, Mass., November 1972.
44. N. M. Tomljanovich, *Ionospheric Ray Tracing and Its Application to R.F. Heating Estimates at Oblique Incidence*, M-73-92, The MITRE Corp., Bedford, Mass., July 1973.
45. J. Parry, *Antenna Patterns—Project COBRA MIST*, Vols. I and II, RADC-TS-TM-72-2, Rome Air Development Center, Air Force Systems Command, Griffiss Air Force Base, N.Y., July 1972.